Journal of Hydrology 664 (2026) 134298

Contents lists available at ScienceDirect

Journal of Hydrology

journal homepage: www.elsevier.com/locate/jhydrol

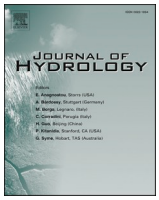

Research papers

Impacts of climate change and human activities on global groundwater storage from 2003 to 2022

Jiawen Zhang *, Tanja Liesch *, Nico Goldscheider

Karlsruhe Institute of Technology (KIT), Institute of Applied Geosciences, Kaiserstr. 12, 76131 Karlsruhe, Germany

ARTICLE INFO

This manuscript was handled by Emmanouil Anagnostou, Editor-in-Chief, with the assistance of Emad Hasan, Associate Editor

Keywords:
GRACE
Groundwater storage change
Drought index
Sustainable groundwater management
Agriculture irrigation

ABSTRACT

Groundwater is integral to land surface processes, significantly influencing water and energy cycles, and it is an important resource for drinking water and ecosystems. Climate change and anthropogenic impacts have an ever-increasing influence on the water cycle and groundwater storage in recent decades. This study leverages GRACE and ERA5-Land data to analyze groundwater storage variability from 2003 to 2022, with a 1° spatial resolution. Approximately 81 % of global regions have shown significant groundwater storage changes, with 48 % experiencing declines and 52 % observing increases. Approximately 3.4 billion people live in regions where groundwater has significantly declined over the past 20 years. Findings indicate considerable global groundwater changes, with depletion hotspots (>20 mm/year) in northern India, the North China Plain, eastern Brazil, and around the Caspian Sea. Standardised Precipitation-Evapotranspiration Index (SPEI) trends exhibit a stronger influence on groundwater storage change than precipitation trends, highlighting the critical role of evapotranspiration. Groundwater depletion is driven primarily by agricultural irrigation and over-abstraction, with population density playing a relatively smaller role. GRACE data facilitates global monitoring, underscoring the need for long-term dynamic observation to inform sustainable groundwater management policies crucial for regions facing groundwater depletion to ensure long-term freshwater resource sustainability.

1. Introduction

Groundwater resources play a crucial role in environmental processes, serving as the primary source of drinking water for 50 % of the world's urban population and around 25 % of all water withdrawn for irrigation (Pointet, 2022). Recent findings reveal that rapid declines in groundwater levels, more than 0.5 m per year, are common in the 21st century, especially in dry areas with extensive cropland (Jasechko et al., 2024). Groundwater depletion due to irrigation is evident in many key agricultural regions (Rodell et al., 2009, 2018; Famiglietti et al., 2011; Voss et al., 2013). Human activities, particularly irrigation, which accounts for 70 % of global water withdrawals and 90 % of water consumption, have a direct impact on these resources (Siebert et al., 2010). Furthermore, 4 billion people face severe water shortages for at least one month each year (Mekonnen & Hoekstra, 2016). This pattern threatens the long-term sustainability of groundwater extraction (Brauman et al., 2016; Wada et al., 2014). Furthermore, excessive groundwater extraction, coupled with irrigation and climate change, could lead to wells running dry (Gleeson et al., 2012; Jasechko & Perrone, 2021). Therefore, analyzing groundwater storage and its fluctuations is crucial to comprehending the effects of climate change and interactions between land and atmosphere.

Groundwater is influenced by both climatic and human activities and exhibits different behaviors in various regions (Amanambu et al., 2020; Padrón et al., 2020; Scanlon et al., 2023). Climate change further stresses groundwater systems through its impacts on precipitation rates and intensity, evapotranspiration (ET), water demand, soil moisture, surface runoff, and glacial conditions, significantly affecting the terrestrial hydrological cycle (Fan et al., 2020; Tabari, 2020; Williams et al., 2020; Condon et al., 2020). These changes result in the redistribution of water resources across spatial and temporal scales, resulting in more frequent and severe agricultural and ecological droughts (Anghileri et al., 2018; Setegn et al., 2011; Legg, 2021). Changes in vegetation alter land use, subsequently affecting the distribution of precipitation among evapotranspiration, surface runoff, and groundwater recharge. Human activities significantly impact groundwater storage through various means, such as the regulation of reservoirs or dams, agricultural irrigation, and industrial and domestic water use. Urbanization and

* Corresponding author.
E-mail addresses: jiawen.zhang@kit.edu (J. Zhang), tanja.liesch@kit.edu (T. Liesch).

https://doi.org/10.1016/j.jhydrol.2025.134298
Received 5 November 2024; Received in revised form 3 August 2025; Accepted 17 September 2025
Available online 20 September 2025

agricultural irrigation further exacerbate regional imbalances in groundwater supply and demand, resulting in water scarcity and notable changes in the spatial and temporal distribution of hydrological processes and water balance elements (Taylor et al., 2013; Joodaki et al., 2014). Understanding the long-term spatiotemporal patterns of groundwater storage changes in response to climate change and human activities is essential for informed groundwater management and protection decisions.

Monitoring and managing groundwater is challenging due to the vast size and hidden nature of aquifers, which are difficult to observe directly, though some remote sensing techniques can provide insights. Typically, local and regional groundwater conditions are assessed through in situ measurements of groundwater levels or water balance estimates (Bhanja et al., 2020). However, comprehensive large-scale data have historically been limited, and direct observations of groundwater level and storage changes have often been constrained by the high cost of data collection and restrictive data policies (Jasechko et al., 2024). In addition to being monitored by in situ well observations, groundwater storage can be simulated by hydrological models. Hydrological models provide an abstract or generalized description of hydrological processes in different regions, enabling the study of the effects of climate change and human activities on these processes. Common global hydrological models include the WaterGAP Global Hydrology Model (WGHM; Herbert & Döll, 2019; Veldkamp et al., 2018) and the PCRaster Global Water Balance (PCR-GLOBWB; Wada et al., 2014; Sutanudjaja et al., 2018). Hydrological model simulations require extensive observational data for input parameters. Variability in these parameters can lead to significant uncertainties in simulated water storage analyses (Qi et al., 2022). Furthermore, limited understanding of groundwater recharge and abstraction processes, coupled with the scarcity of independent ground-based observations for model calibration, further exacerbates these uncertainties (Döll et al., 2014). In recent years, this large-scale information gap has been bridged by utilizing data from the Gravity Recovery and Climate Experiment (GRACE) and its successor, the GRACE Follow-On (GRACE-FO) satellite missions. The advent of the GRACE satellites has substantially improved our understanding of global groundwater storage changes through remote sensing technology at the global scale (Scanlon et al., 2023). Since their launch in 2003, numerous studies have addressed changes in groundwater storage (GWS) derived from GRACE data (Richey et al., 2015; Bhanja et al., 2016; Scanlon et al., 2018; Rateb et al., 2020; Li et al., 2024). However, the use of gravity satellite data has limitations, including low spatial resolution, making it most suitable for regions larger than 200,000 km^2, and low temporal resolution at a monthly scale. Additionally, it is important to address challenges such as difficulties in selecting data from multiple sources (Gao et al., 2023), data gaps (Wang & Zhang, 2024), and low spatiotemporal resolution (Yin et al., 2022).

The reasons for groundwater storage changes vary widely. Overextraction for irrigation is a significant factor contributing to the regional groundwater declination, as observed in California's Central Valley (Famiglietti et al., 2011), the North China Plain (Feng et al., 2017), India (Asoka et al., 2017; Rodell et al., 2009), and the Middle East (Voss et al., 2013). Severe droughts have also led to substantial reductions in groundwater storage, such as in southern and northern Africa (Rodell et al., 2018). The conclusions derived from GRACE regarding changes in groundwater storage mainly focus on individual aquifers or at catchments scale (Joodaki et al., 2014; Chen et al., 2010; Rateb et al., 2020), as well as large global aquifer systems (Thomas et al., 2017; Shamsudduha et al., 2020, Xanke & Liesch, 2022). The release of the HWSA V1.0 database (Zhang et al., 2024) has facilitated high-resolution global-scale assessments of terrestrial water storage anomalies (TWSA) and groundwater storage anomalies (GWSA). However, there has been no recent global-scale study examining the characteristics of groundwater storage changes over the past two decades. Furthermore, there is a lack of global-scale analysis to assess the extent to which human activities and climate change affect groundwater storage across specific regions, such as arid zones, or agricultural areas. Additionally, the driving forces behind changes in regional groundwater storage, as well as their implications at a global scale, remain insufficiently discussed. The main objectives of this study are:

1. Investigation of global trends in groundwater storage from 2003 to 2022.
2. Integration of multiple data sources to examine the relationship between groundwater storage changes, climatic characteristics, and human activities, as well as analysis of the driving mechanisms behind these changes.
3. Regional analysis of significant groundwater storage changes over the past 20 years, attributing these variations to climate change and human activities.

2. Data and methods

2.1. Data on groundwater storage data

The data retrieved from the GRACE/GRACE-FO RL06 Mascon solutions (Save et al., 2016; Save, 2020) provided by the Center for Space Research (CSR) for the period January 2003 to December 2022 were used to isolate gridded groundwater storage changes. The data were resampled from a spatial resolution of 0.25° to 1°. Groundwater storage anomalies were estimated using a mass balance approach, which allows for the isolation of a groundwater storage signal from terrestrial water storage. This approach assumes that groundwater storage (ΔGW) can be computed by subtracting soil moisture (ΔSM), snow water equivalent (ΔSWE), surface water (ΔSWA), canopy water storage (ΔCWS) from total water storage (ΔTWS), as shown in Eq. (1):

$$\Delta GW = \Delta TWS - \Delta SM - \Delta SWE - \Delta SWA - \Delta CWS \quad (1)$$

Soil moisture (ΔSM), snow water equivalent (ΔSWE), surface water (ΔSWA), and canopy water storage (ΔCWS) data were obtained from the ERA5-Land dataset (Muñoz Sabater, 2019; Muñoz Sabater et al., 2021). The ERA5-Land data were used at a monthly temporal resolution and resampled from 0.1° to 1° to align with the CSR GRACE Mascon data. The decision to conduct the analysis at a 1° spatial resolution was made after careful consideration of several key factors: (1) the intrinsic resolution limitations of GRACE data (Wiese et al., 2016); (2) the need for computational efficiency in global-scale trend analyses (Rodell et al., 2018; Scanlon et al., 2018); and (3) the control of error propagation and uncertainties. The 11-month data gap between GRACE and GRACE-FO missions (July 2017 to May 2018) was addressed using the Singular Spectrum Analysis (SSA) method. SSA is a robust technique that decomposes a time series into components ranked by variance, enabling the extraction of non-linear trends and dominant oscillations while effectively reducing noise (Vautard et al., 1992; Hassani, 2007). By applying SSA, we estimated the missing data based on trends observed before and after the gap, ensuring a consistent and reliable dataset. This approach has been extensively validated and employed in previous studies to address GRACE data gaps (Yi & Sneeuw, 2021; Li et al., 2019). In addition to SSA, alternative approaches have been developed to address the data gap between the GRACE and GRACE-FO missions. Notable examples include the methods proposed by Zhang et al. (2022) and Rateb et al. (2022).

This study investigates the impact of environmental changes on global groundwater storage by analyzing eight key indicators, which encompass climate factors, human activities, and other relevant variables (see Table 1). These indicators were selected to capture the complex, multidimensional interactions influencing groundwater storage, enabling a comprehensive assessment of their relationships at the global scale.

Table 1
Datasets of environmental changes affecting global groundwater storage.

Factor	Time span and temporal resolution	Unit	Source
Climate factors			
Precipitation	2003–2022, monthly	mm/a	Harris et al., 2020
Annual potential evapotranspiration	2003–2022, monthly	mm/a	Martens et al., 2017; Miralles et al., 2011
Standardised Precipitation-Evapotranspiration Index (SPEI)	2003–2022, monthly	Unitless	Vicente-Serrano et al., 2010
Human factors			
Population	2003 – 2020, yearly	Number of people	WorldPop, 2018
Groundwater abstraction data	2003 – 2019, monthly	mm/a	Müller Schmied et al., 2021
Area actually irrigated	2005	%	Siebert et al., 2013
Areas equipped for Irrigation with groundwater	2005	%	Siebert et al., 2013
Other factors			
Leaf Area Index (LAI)	2003 to 2022, monthly	%	Myneni et al., 2021

2.2. Data on climate factors

Monthly gridded precipitation data were obtained from the Climatic Research Unit (CRU) (Harris et al., 2020). The aridity index (AI) (Middleton & Thomas, 1997) quantifies climatic dryness and is defined as the ratio of annual precipitation (P) to annual potential evapotranspiration (PET). The PET data used in this study are derived from the Global Land Evaporation Amsterdam Model (GLEAM) (Martens et al., 2017; Miralles et al., 2011). According to the AI index, regions are classified into hyperarid ($AI < 0.05$), arid ($0.05 \leq AI < 0.2$), semiarid ($0.2 \leq AI < 0.5$), and dry subhumid ($0.5 \leq AI < 0.65$) subtypes. The Standardised Precipitation-Evapotranspiration Index (SPEI) is a meteorological drought index used to quantify the severity of drought or wetness in a region. It integrates data on precipitation and potential evapotranspiration (Vicente-Serrano et al., 2010). According to SPEI index, regions are classified into Extremely Wet ($SPEI > 2.0$), Very Wet ($1.5 \leq SPEI \leq 1.99$), Moderate Wet ($1.0 \leq SPEI \leq 1.49$), Normal ($-0.99 \leq SPEI \leq 0.99$), Moderate Dry ($-1.0 \leq SPEI \leq$ -1.49), Very Dry ($-1.5 \leq SPEI \leq$ -1.99), and Extremely Dry ($SPEI < -2.0$). Global maps of monthly Standardised Precipitation-Evapotranspiration Index (SPEI) for the period January 1901 to December 2022 with monthly resolution are available (Beguería et al., 2014). AI primarily quantifies long-term (multi-year average) drought characteristics based on the ratio of precipitation to potential evapotranspiration (PET), thereby capturing the fundamental spatial distribution of climatic aridity. In contrast, SPEI reflects short- and medium-term climate variability, including the impact of recent climate fluctuations such as drought events, making it particularly useful for analyzing the dynamic changes in climatic drought. By integrating both indicators, we can achieve a more comprehensive characterization of climate-induced drought across different temporal scales, mitigating the limitations associated with using a single index.The climate factors cover the period from 2003 to 2022, and the resolution of these datasets has been standardized to $1^\circ \times 1^\circ$ using bilinear interpolation to match the resolution of the GRACE data.

2.3. Data on human factors

Annual population data were collected from WorldPop (WorldPop, 2018) spanning the years 2003 to 2020, produced at a 100 m spatial resolution. Gridded groundwater extraction estimates were characterized using groundwater abstraction data reported by WaterGAP (Müller Schmied et al., 2021). For this study, monthly net groundwater abstraction data covering the period from 2003 to 2019 were selected for analysis, standardized to units of mm/month. Irrigation data were sourced from the Global Map of Irrigation Areas (GMIA) (Siebert et al., 2013), produced at a 5 arc-minute spatial resolution around the year 2005. This dataset consists of two components: area actually irrigated and areas equipped for irrigation with groundwater. It provides the percentage of irrigation, derived by integrating subnational statistics with geospatial data on the location and extent of irrigation schemes. The data mentioned above are not available for the entire study period from 2003 to 2022. Therefore, the data used in this study are selected to align as closely as possible with this timeframe. Furthermore, the resolution of these datasets has been standardized to $1^\circ \times 1^\circ$ through bilinear interpolation to align with the resolution of the GRACE data.

2.4. Data on other factors

Data representing vegetation cover were selected using the monthly Leaf Area Index (LAI) sourced from MOD15A2H (Myneni et al., 2021), spanning the period from 2003 to 2022. These data were included to analyze whether large scale changes in vegetation, especially from deforestation of rainforests, have any influence on GWS.

2.5. Method on trend analysis

Gridded groundwater trends in magnitude and significance were assessed using the Seasonal Mann-Kendall trend test (Hirsch et al., 1982) and the Sen Slope estimator (Sen, 1968). These methods were chosen to mitigate the influence of non-normally distributed variables, particularly those prone to seasonal fluctuations and outliers. The Seasonal Mann-Kendall test evaluates the significance of monotonic trends based on the null hypothesis, distinguishing between significant ($p \leq 0.05$) and non-significant ($p > 0.05$) trends.

2.6. Method on driving force analysis

Attribution studies aim to identify the primary factors driving changes in groundwater storage. Multiple linear regression (MLR) is a widely used statistical method in hydrology and climate sciences for modeling relationships between dependent and independent variables, providing insights into the links among key variables (Seidou et al., 2007; Tibshirani, 1996; Zou & Hastie, 2005; Hoerl & Kennard, 1970). Its ability to establish an initial quantitative framework makes it particularly suitable for identifying dominant drivers when mechanistic models are unavailable or impractical due to data limitations. Therefore, in the context of our large-scale global assessment, MLR serves as a practical and validated method for exploring these relationships. Despite its advantages, the MLR method has several limitations. First, it assumes a linear relationship between dependent and independent variables, which may oversimplify complex real-world processes, especially in hydrology where nonlinear interactions are common (Dormann et al., 2013; Sun et al., 2020). MLR assumes that residuals are normally distributed, independent, and homoscedastic; violations of these assumptions can lead to biased or inefficient estimates (Kutner, 2005). Moreover, MLR cannot capture dynamic feedbacks and time-dependent processes that may be critical in groundwater systems.

The objective of our attribution analysis is to determine which driving factors contribute to the observed changes in groundwater storage and to quantify their respective contributions in either a quantitative or semi-quantitative manner. This study focuses specifically on assessing the roles of climate variability and human activities in influencing global groundwater storage changes, rather than addressing highly nonlinear, localized interactions. At the global scale, complex nonlinearities among drivers are often averaged out, leading to

relationships that approximate linear patterns. Thus, MLR remains an appropriate and effective tool for yielding valuable quantitative insights and for identifying the primary factors influencing groundwater storage dynamics (Jyolsna et al., 2021; Rajaee et al., 2019).

The general purpose of MLR is to better understand the relationship between multiple independent (predictor) variables and a dependent (criterion) variable (Yilmaz & Yuksek, 2008), as expressed in Eq. (2):

$$Y = a + b_1 \times x_1 + b_2 \times x_2 + b_3 \times x_3 + \cdots b_n \times x_n + \in \quad (2)$$

where Y is the dependent variable, x_1, x_2, …x_n are the independent variables, b_1, b_2, … b_n are regression coefficient. The regression coefficients represent the independent contributions of each independent variable to the prediction of the dependent variable. In this study, MLR is applied to analyze groundwater storage responses to climatic factors and human activities, including trends in precipitation, drought, population density, irrigation conditions, and groundwater abstraction, to identify the main drivers of groundwater storage changes. The ultimate goal is to determine whether observed trends are primarily due to climate impacts, human impact, or a combination of both. Additionally, trends for specific factors were calculated and compared mathematically, with detailed analysis conducted on specific regions.

3. Results and discussion

3.1. Trends in groundwater storage and validation

Fig. 1 illustrates the spatial distribution of the mean annual groundwater storage change trend from 2003 to 2022. The following regions were excluded: Antarctica, Greenland, the Gulf of Alaska coast, the Canadian Archipelago, and the Patagonian ice fields. The primary reason is that changes in water storage in these regions are mainly due to ice-sheet and glacier ablation caused by a warming climate, rather than changes in groundwater reserves (Rodell et al., 2018; Velicogna et al., 2014).

Over the past two decades, groundwater storage has exhibited spatial heterogeneity, with most depletion occurring within the Earth's mid-latitudes. With a 95 % confidence level, approximately 81 % of global regions, excluding ice melt regions, have experienced a significant trend in groundwater storage. Of these regions, 48 % have witnessed a decline in groundwater levels, whereas 52 % have experienced an increase. Approximately 3.4 billion people live in regions where groundwater levels have significantly declined over the past 20 years. Notably, a significant decline in groundwater storage (>20 mm/a) was observed in northern India, eastern Brazil, and areas surrounding the Caspian Sea. Among these, the most severe groundwater depletion occurred in the regions around the Aral, the Caspian Sea and northern India, with an average annual decline exceeding 30 mm over the past 20 years. These areas are characterized by sparse vegetation and fragile ecological environments. Examples of areas with rising groundwater storage (GWS) trends include West and Central Africa, the Amazon rainforest, the Great Lakes region and the area west of the Great Lakes, with groundwater increases exceeding 20 mm annually. This significant increase in groundwater storage is likely due to high average precipitation, dense surface vegetation, and prevailing wetting climate trends (Green et al, 2011; Amanambu et al., 2020). Additionally, groundwater depletion is more pronounced in areas where water tables are already deep (Fan et al., 2013). In such regions, further depletion can exacerbate the challenge of accessing groundwater, potentially requiring the construction of deeper wells, which increases costs (Jasechko & Perrone, 2021).

3.2. GWS and climate

3.2.1. Precipitation

The correlation between precipitation and groundwater storage has been confirmed in multiple studies (Thomas & Famiglietti, 2019; Russo & Lall, 2017). As shown in Fig. 2, precipitation trends exhibit an uneven spatial distribution. The most significant increases in precipitation are observed in the eastern United States, northern Russia, central Africa, and southern China, while marked decreases are primarily concentrated in South America. Despite the notable reduction in precipitation in South America, most regions do not show a corresponding decline in groundwater storage. For instance, in the Amazon rainforest, even though precipitation is decreasing, high average temperatures and high average precipitation have not prevented the trend of rising

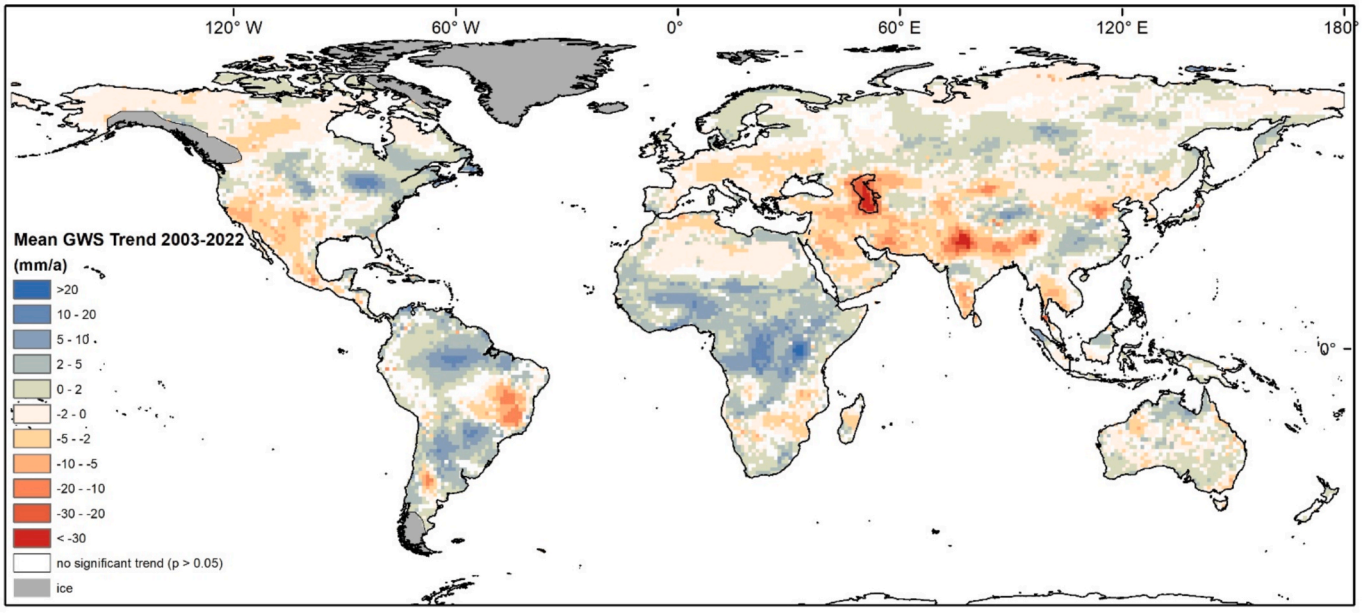

Fig. 1. Mean annual trends of GRACE-derived global GWS for the period of 2003–2022 (mm/a). Red areas indicate regions with declining groundwater storage, while blue areas show regions with increases All calculations use the original dataset resolution of 1°, with colored areas in the figure representing statistically significant trends at the 95% confidence level. (For interpretation of the references to colour in this figure legend, the reader is referred to the web version of this article.)

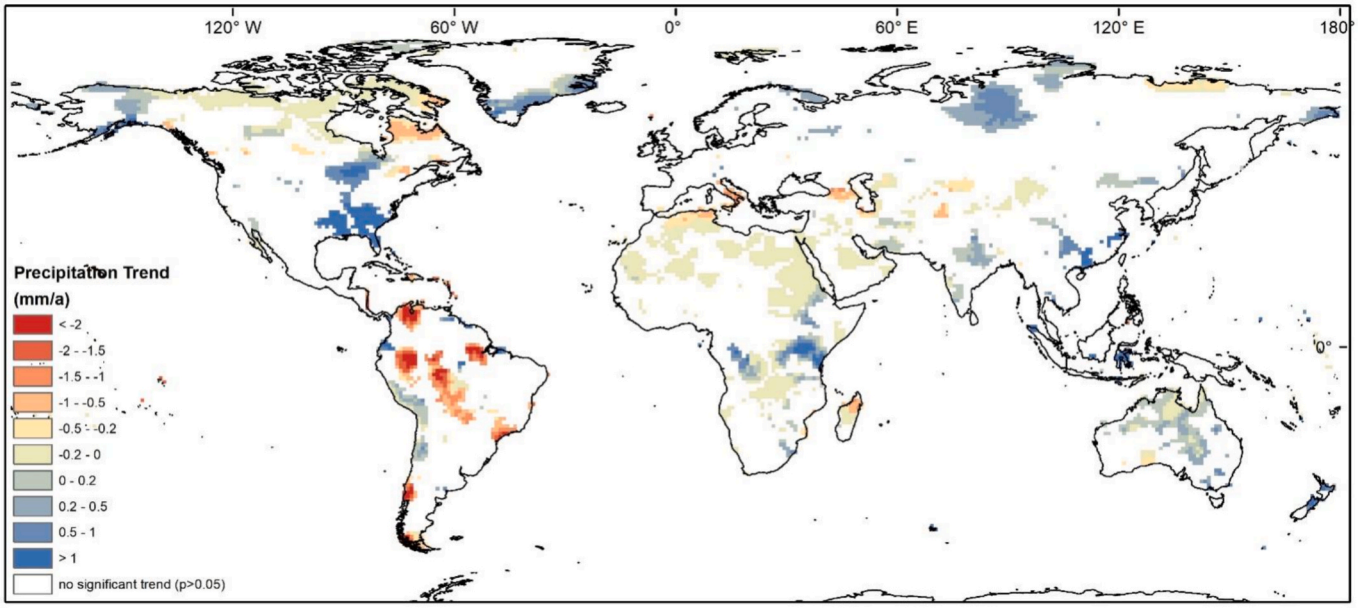

Fig. 2. Mean annual trend of precipitation for the period of 2003–2022 (mm/a), the colored areas in the figure indicate significant trends at the 95% confidence level.

groundwater storage (Heerspink et al., 2020). Although changes in precipitation can affect groundwater recharge, variations in groundwater storage do not always directly correspond to changes in precipitation. Fig. 3 shows the global distribution of multi-year average precipitation. Compared to precipitation trend maps, the average precipitation map is more spatially correlated with the groundwater storage distribution map. Therefore, the increase or decrease in precipitation is not the sole factor influencing groundwater storage, emphasizes the impact of evapotranspiration on groundwater storage. Long-term precipitation changes may impact global groundwater storage due to the slow response to recharge, and many regions experience groundwater decline due to excessive extraction (Herrera-Pantoja & Hiscock, 2008; Thomas & Famiglietti 2019). Increased evapotranspiration due to climate change may prevent groundwater reserves from being replenished by precipitation, even if precipitation increases (Green et al., 2011).

3.2.2. *SPEI drought index*

The spatial distribution of the trend of the global SPEI trend over the past 20 years is shown in Fig. 4. The climatological mean Standardized Precipitation-Evapotranspiration Index (SPEI), representing meteorological drought conditions for the period from 2003 to 2022, is shown in the Fig. 5.Compared to the precipitation trends shown in Fig. 2, changes in groundwater storage are more closely aligned with the spatial distribution of the SPEI trend. This relationship has also been observed by Dai (2013) and Wang et al., (2015). The likely reason is that SPEI accounts for multiple factors, including precipitation, temperature, evapotranspiration, and other climatic conditions. Therefore, it highlights the significant role of evapotranspiration in influencing groundwater storage. Van Loon (2015) noted that groundwater storage

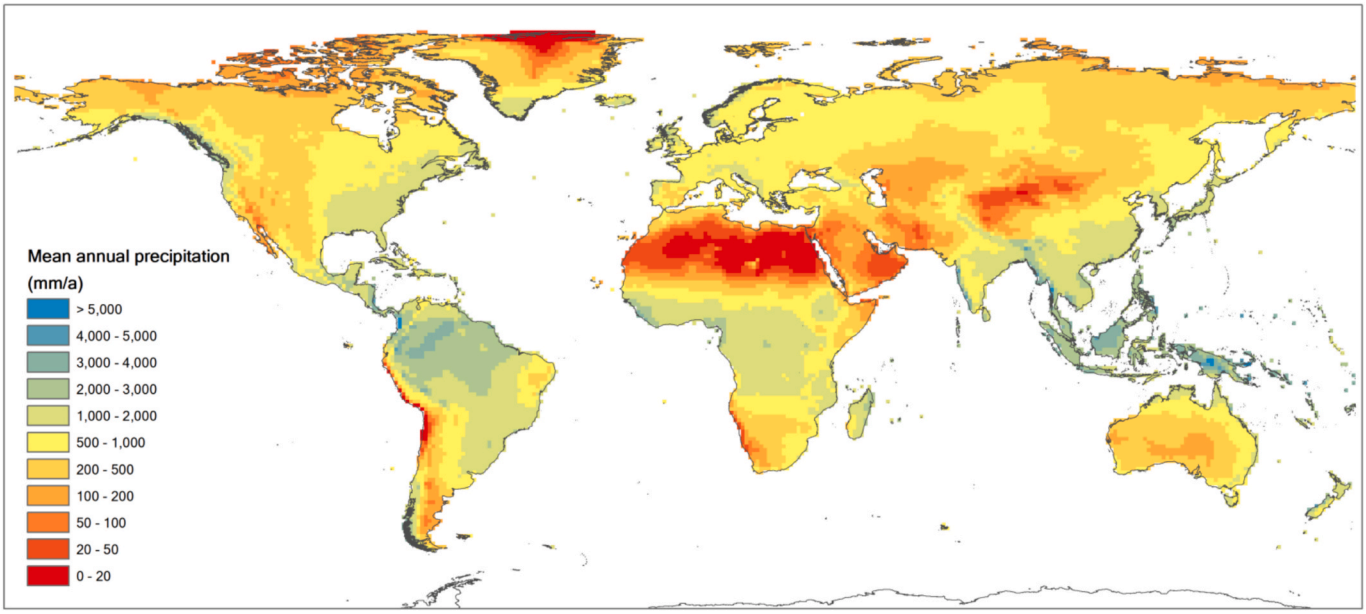

Fig. 3. Mean annual precipitation for the period of 2003–2022 (mm/a).

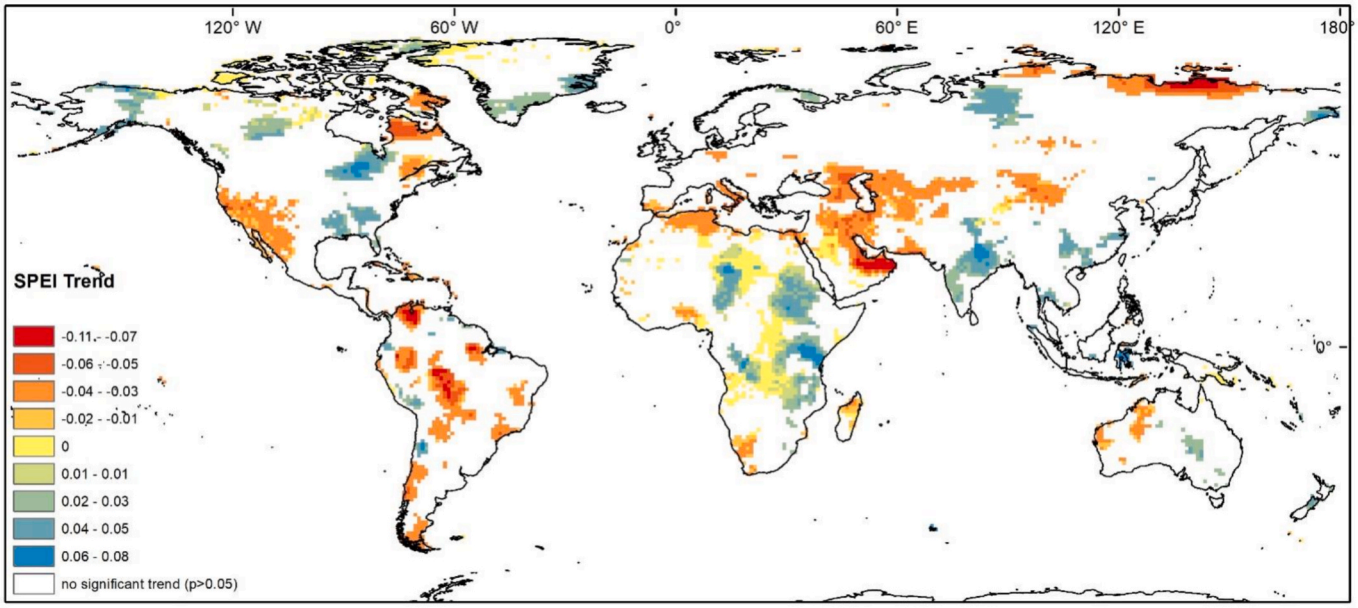

Fig. 4. Mean annual trend of Standardised Precipitation-Evapotranspiration Index (SPEI) for the period of 2003–2022, the colored areas in the figure indicate significant trends at the 95% confidence level.

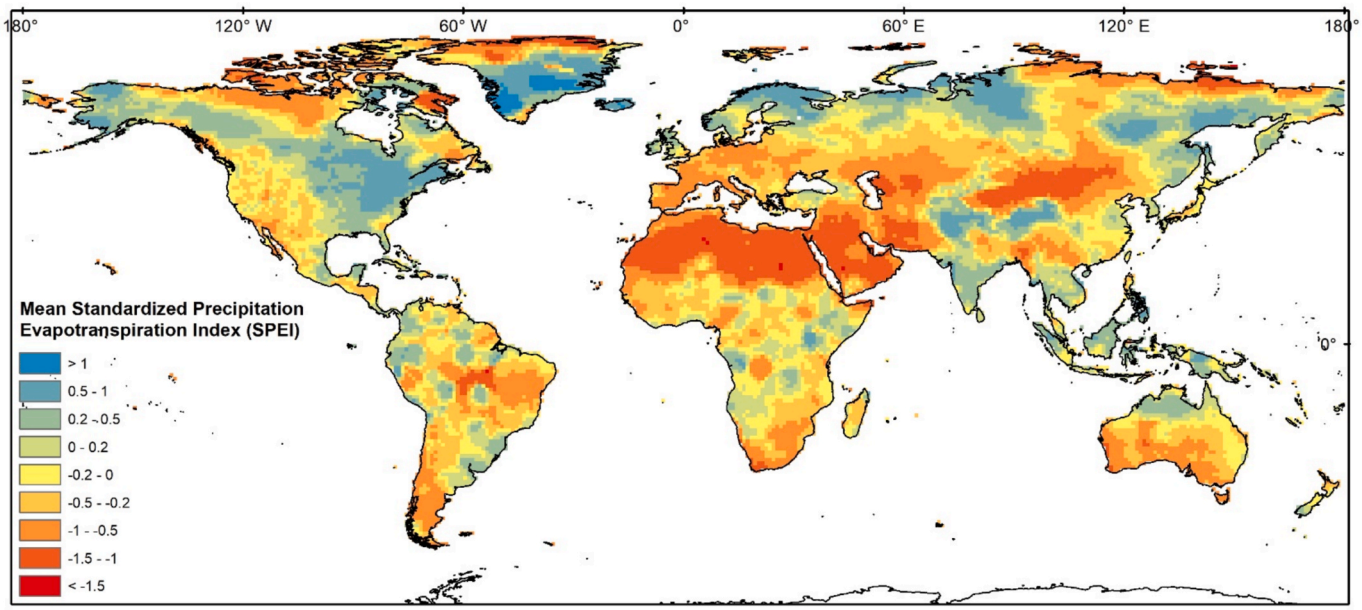

Fig. 5. Mean annual standardized precipitation evapotranspiration index (SPEI) for the period of 2003–2022.

fluctuates in response to meteorological trends, increasing during wetter periods and decreasing during drier periods. However, not every meteorological drought leads to a decline in groundwater levels. This is mainly because short-term meteorological droughts do not impact groundwater, and only prolonged droughts cause significant changes in groundwater storage (Li & Rodell, 2015; Barichivich et al., 2019). Additionally, groundwater droughts exhibit a delayed effect compared to meteorological droughts, as it takes time for precipitation to recharge groundwater, and a reduction in precipitation leading to meteorological drought does not immediately cause groundwater depletion (Han et al., 2019; Gates et al., 2011).

3.2.3. *Aridity index*

The climatological mean Aridity index (AI), representing the climatological state for the period from 2003 to 2022, is shown in Fig. 6. Since groundwater storage largely depends on both climatic conditions and topography, we focus on the long-term perspective, where climate exerts a stronger influence. Therefore, the mean trends of annual groundwater storage and the percentage of area with declining groundwater storage across different Aridity Index classes, plotted against the climatological mean AI, are presented in Fig. 7. The analysis shows that the most significant groundwater decline occurred within the AI range of 0.1 to 0.5, peaking at 0.1 to 0.2. This indicates that arid and semi-arid areas (see Methods), rather than hyper-arid region, are experiencing the greatest depletion, a fact that has also been found by Scanlon et al. (2023).

The Sahara Desert, which has an AI below 0.1 and lacks vegetation, is not typically dependent on groundwater, and thus does not significantly

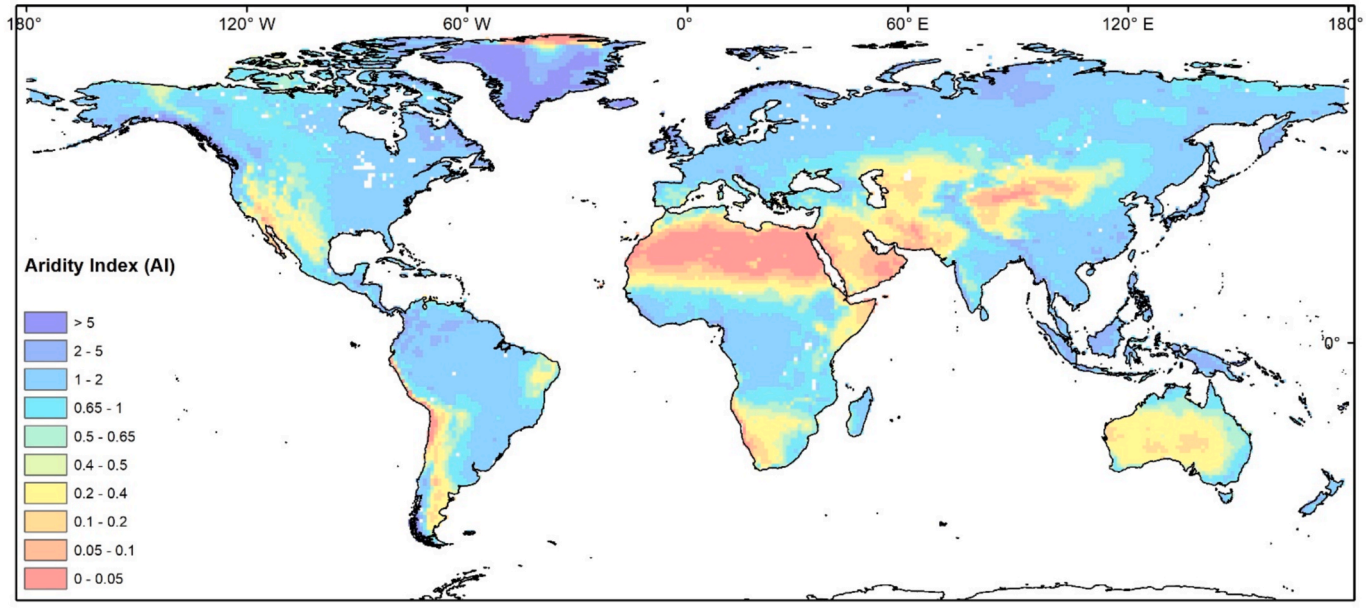

Fig. 6. Global Aridity Index (AI) for the period of 2003–2022.

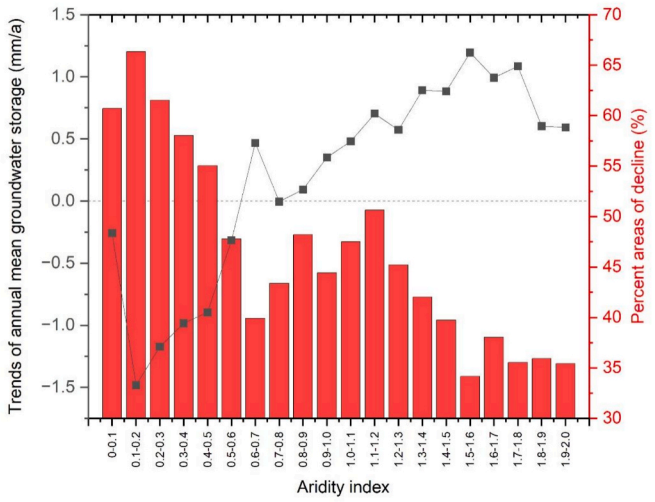

Fig. 7. Mean trends of annual groundwater storage (black line) and the percentage of area with declining groundwater storage across different Aridity Index classes (bars) plotted against the climatological mean AI (except the ice melt regions). The climatological mean AI on the x axis is the annual mean AI for the period from 2003 to 2023.

contribute to this extreme phenomenon (Rohde et al., 2024). Excluding the Sahara Desert from the analysis did not substantially alter the groundwater storage trends, suggesting it is not a primary factor in substantial groundwater depletion, a fact that has also been found by Cuthbert et al. (2019). In arid and semi-arid regions, more than 60 % of areas showed groundwater decline trends, indicating that these regions play a dominant role in both the area and intensity of groundwater depletion.

Overall, the observed groundwater distribution trends indicate that groundwater storage are declining in arid and semi-arid regions, while increasing in humid regions (AI $\geq$ 0.8). This disparity may lead to a more uneven distribution of groundwater.

3.3. GWS and human factors

Regarding the impact of human activity on groundwater storage trends, we examined four human activity related factors as illustrated in Fig. 8. These factors are: (a) area actually irrigated (%), (b) areas equipped for irrigation with groundwater (%), (c) annual mean net abstraction from groundwater (mm/a), and (d) population density (per/km^2). For Fig. 8(a), when the proportion of the actually irrigated area is below 50 %, the trend in groundwater storage is not conspicuous. However, as the proportion increases from 50 % to 90 %, a discernible decline in groundwater levels becomes evident in more and more areas, with many of them experiencing a decrease of approximately 10 mm per year. Upon surpassing the 90 % threshold, more areas exhibit a pronounced downward trend in groundwater levels, with many regions experiencing declines exceeding 10 mm per year. This also includes the regions with the most pronounced declines of more than 20 up to 50 mm/a. Fig. 8(b) shows that many regions with varying proportions of irrigation using groundwater all exhibit significant areas with declines in groundwater storage, most of them in regions with 20 % or more area equipped for irrigation with groundwater, while there are also some regions with high declines and no or little irrigation with groundwater. This may be related to regional recharge and discharge rates, making the relationship between areas equipped for irrigation with groundwater and groundwater storage not so clear. For Fig. 8(c), the data indicate that net recharge to groundwater (negative values of net abstraction, caused by irrigation return flow in areas irrigated by surface water) does not necessarily lead to an increase in groundwater storage, but excessive groundwater abstraction most often results in a decrease in groundwater storage. Different to irrigation and abstraction factors, population density (Fig. 8 (d)) does not have a direct relationship with groundwater storage. Thus, high population density does not necessarily lead to reduced groundwater storage. This confirms that abstractions connected with high population density, e.g. for drinking water or industrial purposes, have a minor effect on GWS, compared to agriculture, which is the cause for the majority of abstracted groundwater and is more likely to be found in less populated regions.

3.4. GWS and vegetation cover

To analyze the potential impacts of vegetation cover and its changes, particularly due to rainforest deforestation, on groundwater storage

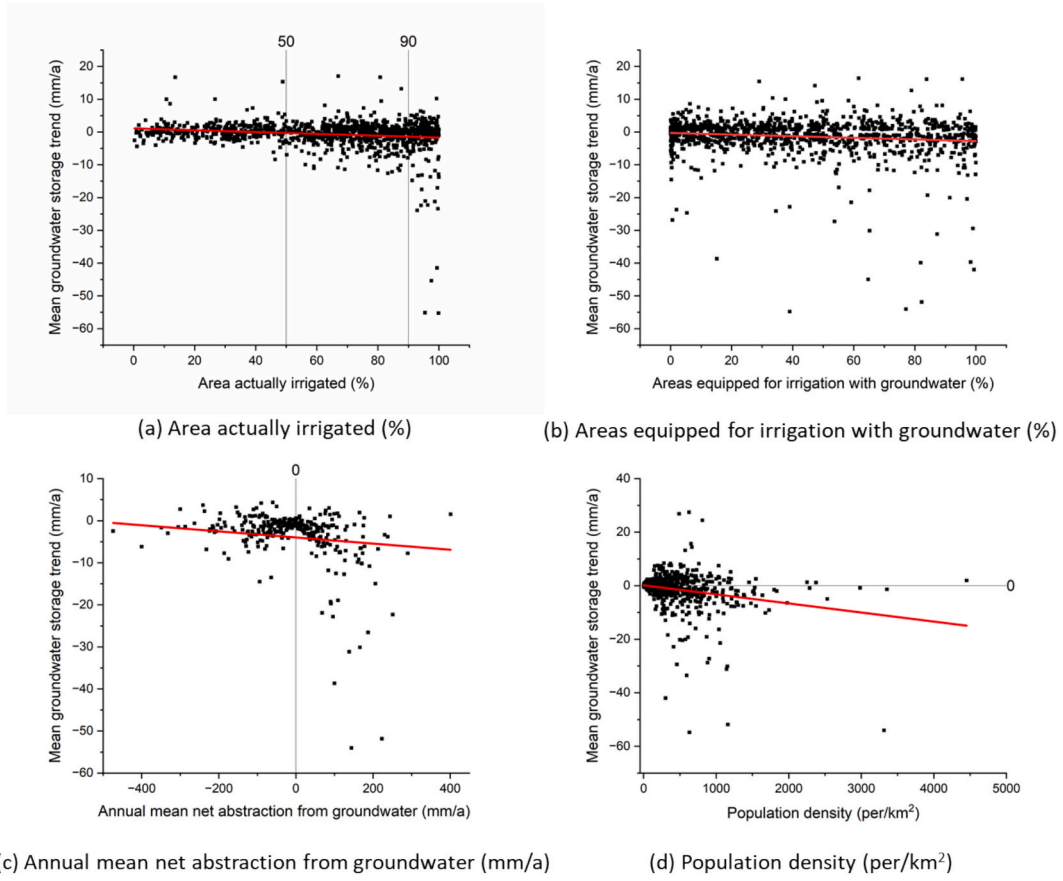

Fig. 8. Mean GWS plotted against four possible factors of human impact, (a) area actually irrigated (%), (b) areas equipped for irrigation with groundwater (%), (c) annual mean net abstraction from groundwater (mm/a), and (d) population density (per/km^2).

(GWS), we compared GWS trends with the mean leaf area index (LAI) (Fig. 9) and LAI trends from 2003 to 2022 (Fig. 10). In recent years, researchers have observed a global greening trend in vegetation using earth observation technologies and remote sensing imagery (Keenan & Riley, 2018; Song et al., 2018), similar to the greening trend observed in the LAI trend discussed in this paper. However, on a global scale, these patterns are not immediately apparent. Regions exhibiting increasing or decreasing GWS trends are found in areas with both high and low LAI, as well as in regions with both increasing and decreasing LAI trends (Tao et al., 2020). Therefore, we discuss the potential influences in selected

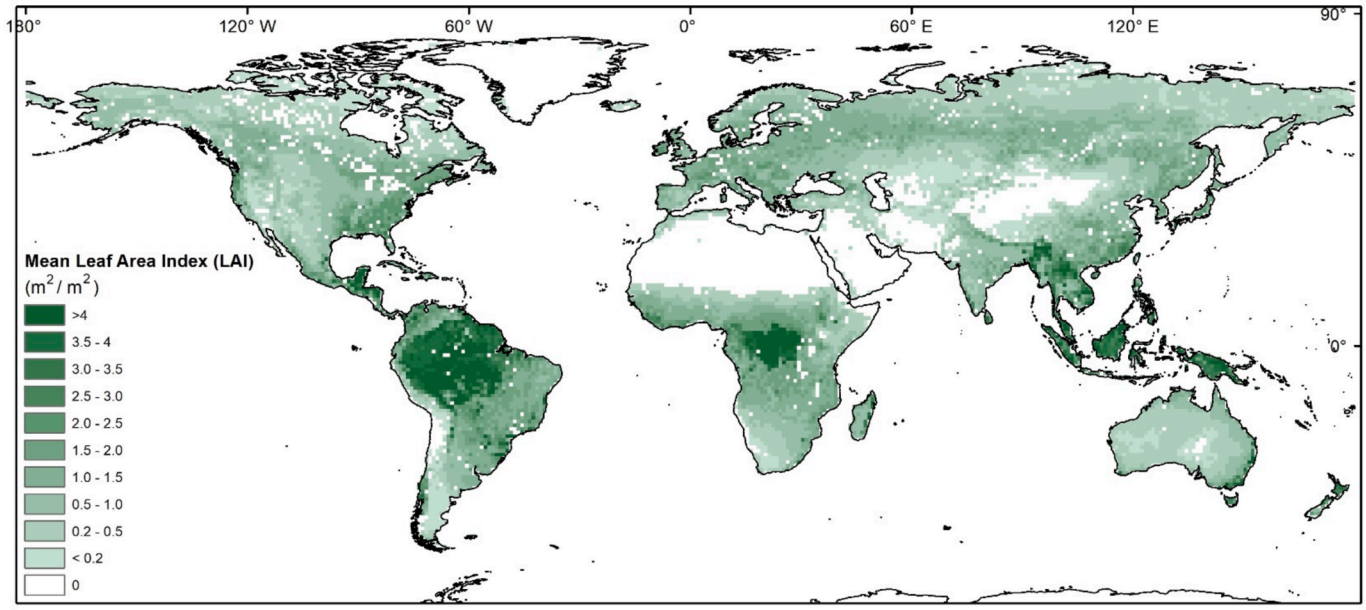

Fig. 9. Mean annual leaf area index (LAI) for the period of 2003–2022 (m^2/m^2).

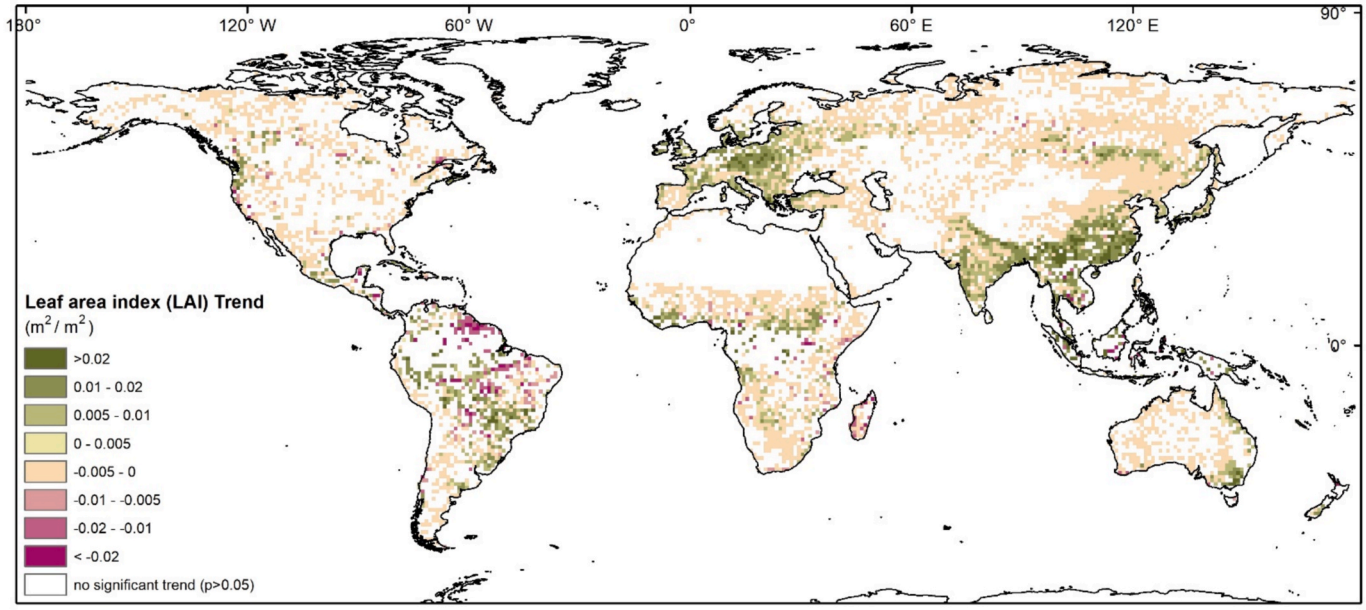

Fig. 10. Mean annual trend of leaf area index (LAI) for the period of 2003–2022(m^2/m^2), the colored areas in the figure indicate significant trends at the 95% confidence level.

regions below.

3.5. Regional groundwater storage changes and attributions

To better understand the drivers of regional groundwater storage (GWS) changes, we applied the Hot Spot Analysis method. This spatial statistical technique identifies statistically significant clusters of high values and low values based on the spatial distribution of the data. In this study, areas in the GWS map where absolute changes exceeded 5 mm/year were first selected. Subsequently, regions with adjacent

Table 2
Statistics of groundwater storage trends and possible influencing factors for the selected regions in Fig. 6. Supposed main driving forces are not directly concluded from the statistics but discussed in the text. Mean Precipitation trend (mm/a): PT, Annual Mean Precipitation (mm/a): MP, SPEI trend: ST, Areas equipped for irrigation (%): I; Area equipped for irrigation with groundwater (%): IG, Population density (people/km^2): POP, Annual net abstraction from groundwater max value (mm/a): GA, climate impact: C, human impact: H, climate and human impact: both.

Region No.	Location	Area (km^2)	Mean GWS trend (mm/a)	GWS trend extreme value (mm/a)	PT (mm/a)	MP (mm/a)	ST	I (%)	IG (%)	POP (people/km^2)	GA (mm/a)	Supposed main driving force
1	Western America	4,241,546	−3.0	−12.7	0.00	574	−0.017	49.7	30.2	63	177.2	Both
2	Central Canada	1,525,571	−1.9	−6.3	−0.03	436	0.008	3.7	0.1	2	3.2	C
3	Eastern United States	906,647	5.4	16.4	0.46	996	0.013	37.9	32.5	94	35.4	C
4	Amazon	2,716,443	4.7	14.1	−0.53	2361	−0.013	12.0	4.2	7	3.9	C
5	Eastern Brazil	1,831,986	−5.2	−17.9	−0.15	1374	−0.016	87.5	18.9	23	32.2	Both
6	Southern Brazil-Paraguay region	1,553,784	5.0	12.3	−0.17	1059	−0.010	42.0	13.3	20	24.6	C
7	Central Argentina	369,510	−3.5	−11.4	0.01	328	−0.009	12.6	1.6	8	0.5	H
8	Central Europe	3,711,950	−1.9	−5.0	0.00	704	−0.013	23.4	16.5	119	244.4	C
9	Northern Africa	2,273,262	−1.6	−7.3	−0.08	95	−0.011	9.4	6.2	21	139.9	Both
10	Western Africa	2,477,929	4.9	14.8	−0.01	1374	0.003	4.0	0.9	80	22.4	C
11	Nile headwaters	3,451,624	6.9	28.2	0.20	1368	0.012	2.8	0.3	78	3.3	Both
12	Southeastern Africa	1,802,587	−2.1	−7.2	0.00	649	0.005	7.8	0.6	32	2.4	H
13	Aral Sea and Caspian Sea	5,708,583	−5.8	−40.4	−0.09	308	−0.025	22.4	13.3	65	101.9	Both
14	Northwestern China	898,833	−3.0	−14.7	−0.06	195	−0.020	20.5	4.4	20	19.8	Both
15	Tibetan Plateau	230,001	5.5	10.7	0.00	154	0.001	0.0	0.0	1	0.0	C
16	North China Plain	1,004,133	−3.4	−16.3	0.02	397	−0.008	43.7	30.2	208	290.3	H
17	Northeast China	966,799	−1.7	−5.0	0.12	635	0.009	61.1	36.4	141	68.8	H
18	Arabian Peninsula	1,754,517	−2.9	−9.3	0.00	113	−0.017	7.4	9.2	62	169.3	Both
19	Northern India	1,532,713	−9.9	−54.8	0.08	602	0.012	59.8	36.5	363	251.6	H
20	Southern India	434,225	−4.8	−11.7	0.08	1100	0.017	77.1	57.9	447	173.9	H
21	South Asia	1,198,228	−5.6	−25.2	−0.02	1200	0.012	49.5	19.9	399	238.4	C
22	Eastern Central China	461,212	3.6	5.4	0.47	1202	0.023	71.3	0.1	295	−0.1	C
23	Mainland Southeast Asia	710,066	−3.3	−9.7	0.18	1846	0.012	49.8	3.0	145	0.5	Both

areas showing similar trends were grouped together, resulting in the identification of 23 distinct regions. To investigate the causes behind these changes, we compiled several potential influencing factors, as detailed in Table 2. Trends and extreme values in groundwater storage were calculated using area-weighted mean values and extremes for each region (maximum values for regions with rising groundwater and minimum values for those with declining groundwater). The proportion of irrigated land was calculated by area-weighting pixel values of irrigation intensity across each study region. Spatial variation maps for these factors include precipitation trends in Fig. 2, annual mean precipitation in Fig. 3, SPEI trends in Fig. 4, mean leaf area index (LAI) and its trends in Figs. 9 and 10, annual mean population density in Fig. 11, and annual mean net groundwater extraction in Fig. 12. To evaluate the impact of each factor on GWS, we conducted a regression analysis to calculate the coefficients, where larger absolute values denote stronger influence. Positive coefficients indicate positive effects, while negative coefficients indicate negative effects (see Fig. 13). Based on these results, we attributed groundwater storage trends to "mainly climate impact," "potential human impact," or a "combination of both." Fig. 14 illustrates the global distribution of 23 regions where significant changes in groundwater storage were observed from 2003 to 2022. The main drivers of these changes were inferred from the specific conditions of each region and the outcomes of regression analysis.

3.6. North America

A historically severe drought that began in 2011–2014 (Griffin & Anchukaitis 2014) and has persisted to the present in Western America (region 1), is centered in southern California and extends into Mexico. This drought period is characterized by a low meanSPEI and a downward trend in SPEI values, indicating continuous aridification (Alam et al., 2021). This has resulted in a mean groundwater storage (GWS) decline of −3 mm/a and an increased groundwater demand, with net abstraction reaching a maximum of 177 mm/a. Approximately 50 % of the surface area is used for agriculture, with 30 % of this agricultural land irrigated using groundwater, supporting a population of 268 million people. Consequently, the decline in groundwater levels is due to a combination of drought and agricultural water demands that exceed renewable water resources.

From 2003 to 2022, overall precipitation has been slightly decreasing, leading to an average GWS decline of −1.9 mm/a in Central Canada (region 2). This loss of water aligns with a recent study concluding that Canada's subarctic lakes are vulnerable to drying when snow cover declines (Bouchard et al., 2013). Moreover, there is hardly any abstraction from groundwater connected to irrigation. Therefore, the changes are supposed to be climate-related.

The increasing precipitation trend in the Eastern United States (region 3) has led to a significant rise in groundwater storage (Rateb et al., 2020), with an average increase of 5.4 mm/a and a maximum increase of 16.4 mm/a. In this region, 38 % of the land is used for irrigation, mostly relying on groundwater. However, the increase in groundwater levels due to the wetter climate persists despite the extensive use of groundwater for irrigation.

3.7. South America

Despite the decreasing trend in precipitation and significant deforestation in the Amazon (region 4) over the past few decades (Lin et al., 2016), the region still receives an average annual rainfall of 2362 mm, making it one of the most precipitation-rich areas globally. During these two decades, GWS in central and western Brazil and its neighboring areas increased at an average rate of 4.7 mm/a, with a maximum increase of 14.1 mm/a. This trend is attributed to changes of the Amazon water cycle, which has been significantly altered by changes in climate, land cover (especially deforestation, as supported also by a negative trend in the LAI), sea surface temperature and precipitation patterns since the 1980′s (Heerspink et al., 2020; Satizábal-Alarcón et al., 2024).

Eastern Brazil (region 5) has recently experienced a severe drought (Lima et al., 2022), characterized by a significant decrease in the SPEI values and reduced precipitation. This phenomenon is likely associated with a strong El Niño event (Santos et al., 2021). In fact, 2015 was the driest year in the past 37 years (Marengo et al., 2017). Consequently, GWS over the past 20 years has decreased by 5.2 mm/a, with a maximum decline of 17.9 mm/a. This region's challenges result from a combination of human impacts and severe drought. Agriculture occupies 88 % of the area, with most of it dependent on rainfed agriculture.

Groundwater storage has shown significant increases over the past two decades in southern Brazil and adjacent regions in Paraguay (region 6). On average, GWS has increased by 5 mm/a, with a maximum increase of 12.3 mm/a. Despite a decreasing trend in precipitation, the

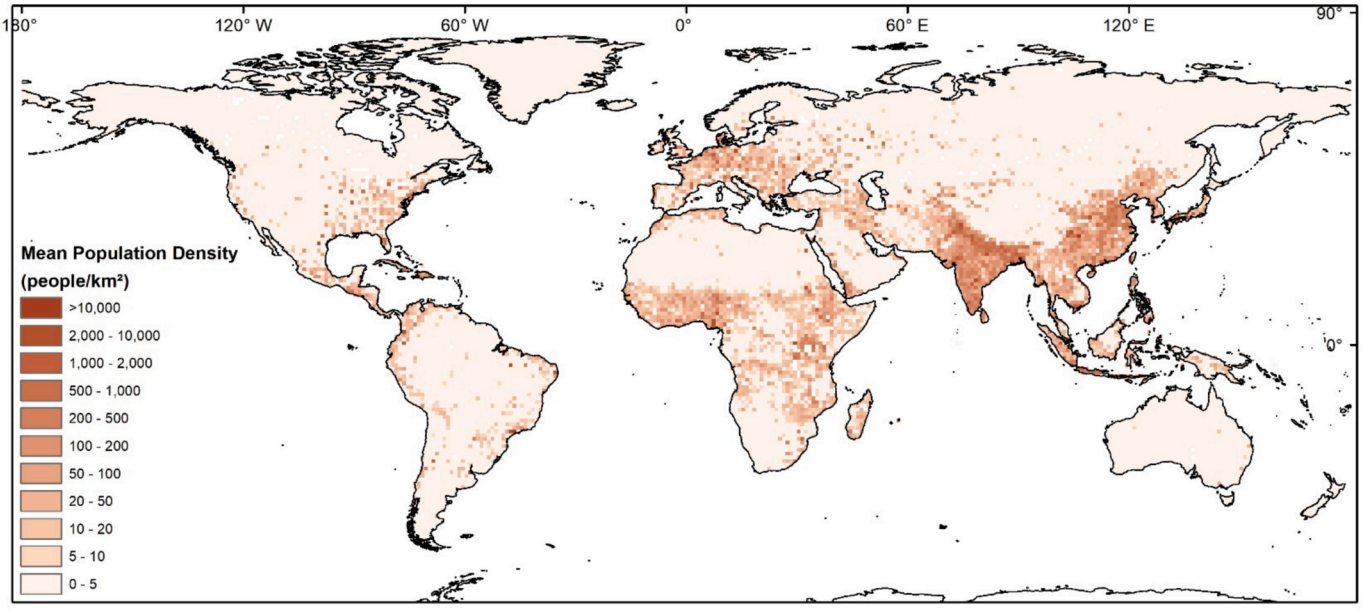

Fig. 11. Mean annual population density for the period of 2003–2020 (people/km^2).

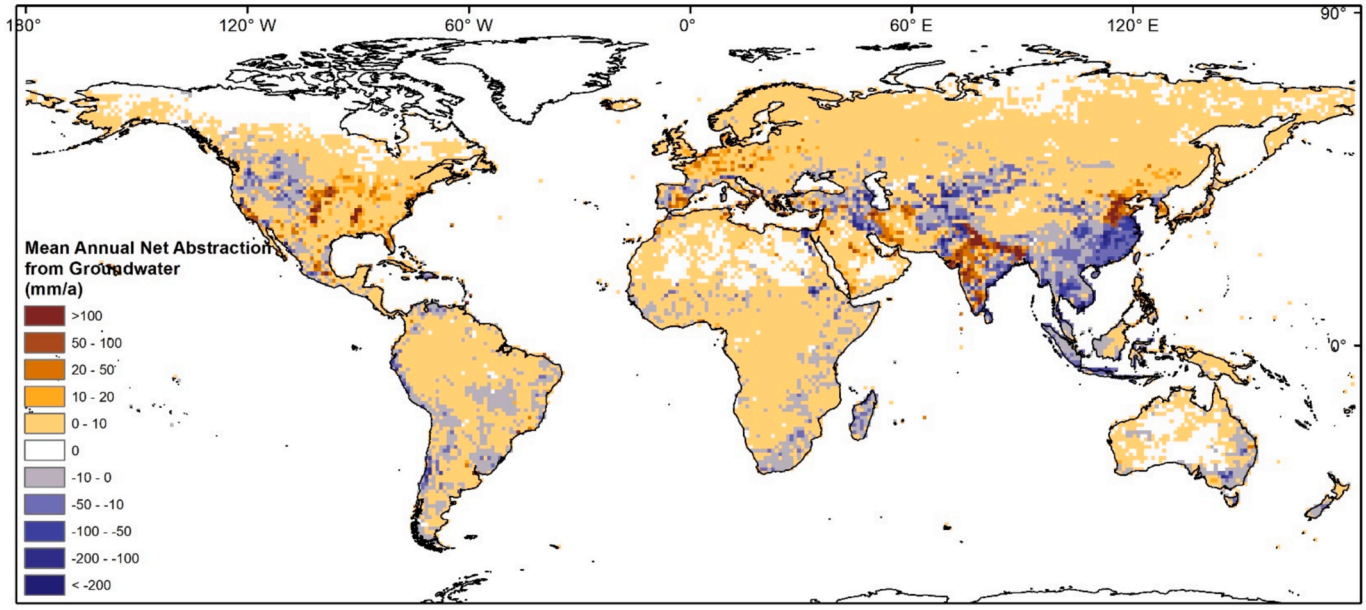

Fig. 12. Mean annual net abstraction from groundwater for the period of 2003–2020 (mm/a).

SPEI values indicate a gradual shift towards a drought climate.

Groundwater storage in Central Argentina (region 7) had previously been declining at a rate of −3.5 mm/a, with the maximum decline reaching −11.4 mm/a. Vegetation in central Argentina is sparse, with a mean Leaf Area Index (LAI) of only 0.33 %. A multi-year drought that began in 2009 has persisted to the present (Müller et al., 2017). Regression results indicate that the primary driver of groundwater storage decline in this region is irrigation.

3.8. Europe

An analysis of the mean annual trends over the study period reveals a slight decrease in GWS in many European countries, with an average value of −1.9 mm/a for Central Europe (region 8). The maximum annual net abstraction from groundwater reached 244 mm/a, which supports 16 % of agricultural activities and 443 million people. Concurrently, extreme drought events over the past 20 years (e.g., 2003, 2011–2013, 2015–2016) (Ionita et al., 2021; Van Lanen et al., 2016) have also influenced the distribution of groundwater reserves. That is depicted also in negative trend of the SPEI in parts of the region, e.g. northern Germany. The results clearly indicate medium-term groundwater stress in most European countries (Xanke & Liesch 2022).

3.9. Africa

During the study period, a severe drought occurred in Northern Africa (region 9) (Spinoni et al., 2019), closely aligning with areas experiencing groundwater depletion. The region exhibited a weak negative trend with an average decrease of −1.6 mm/a. Sparse abstraction regions are concentrated in densely populated areas, with the highest abstraction from groundwater at 140 mm/a, supporting 6 % of irrigation from groundwater and 48 million people. Therefore, the primary cause of groundwater depletion is attributed to meteorological drought and abstraction from groundwater.

Groundwater storage in the tropical climate of Western Africa (region 10) has been increasing at an average rate of 4.9 mm/year. The maximum groundwater abstraction of 22 mm/a supports a population of 199 million people and a small amount of agricultural land. Additionally, the relatively abundant mean annual precipitation (1374 mm/year) and the construction of dams (Scanlon et al., 2022; Zarfl et al., 2015) may contribute to the accumulation of groundwater storage. In addition, land-use change has also been noted as an important driver of groundwater storage trends (Yira et al., 2016).

The groundwater level in Nile headwaters (region 11) has experienced the largest increase globally, with a maximum groundwater storage (GWS) rise of 28.2 mm/a and mean rise of 6.9 mm/a. Despite a large population of 270 million, the maximum abstraction amount is only 3.27 mm/a. This suggests that increased precipitation (positive Precipitation trend of 0.2 mm/a and wetter climate) is the primary driver of GWS variations. Additionally, the management of large lakes and dam construction (Ahmed et al., 2014) in the northern part of the region could also contribute to these changes (Kebede et al., 2017).

The negative trend along the southeastern coast of Africa (region 12) has resulted in an average groundwater storage decline of −2.1 mm/a. This event was associated with a pronounced north–south dipole pattern of positive or negative rainfall and water balance anomalies, typical of the El Niño–Southern Oscillation (ENSO) teleconnection to the region (Kolusu et al., 2019; Scanlon et al., 2022).

3.10. Asia

The demise of the Aral Sea and Caspian Sea (region 13) has been extensively documented in numerous studies (Qadir et al., 2009; Hu et al., 2022). Our estimates indicate a mean groundwater storage (GWS) depletion rate of −5.8 mm/year, with a maximum recorded rate of −40.4 mm/year. This area represents the second-largest groundwater depletion region globally, characterized by both its vast expanse and significant depth of the groundwater depression. The primary climate type in this region is arid, with desert precipitation. Concurrently, the area experiences a high abstraction rate, reaching up to 102 mm/a to support approximately 369 million people. Precipitation in this region is minimal and continues to decrease (as depicted by a negative P trend), contributing to worsening drought conditions. Approximately 22 % of the land is equipped for irrigation, with 13 % of the irrigation relying on groundwater. Therefore, the decline in groundwater levels is attributed to both climate impact and human activity.

During the study period, the groundwater storage in Northwestern China (region 14) decreased by 3 mm/a, with a maximum decrease of 14.7 mm/a. This decline may be related to ice melt from the Tien Shan mountains (Jacob et al., 2012). In this region, 20 % of the area consists

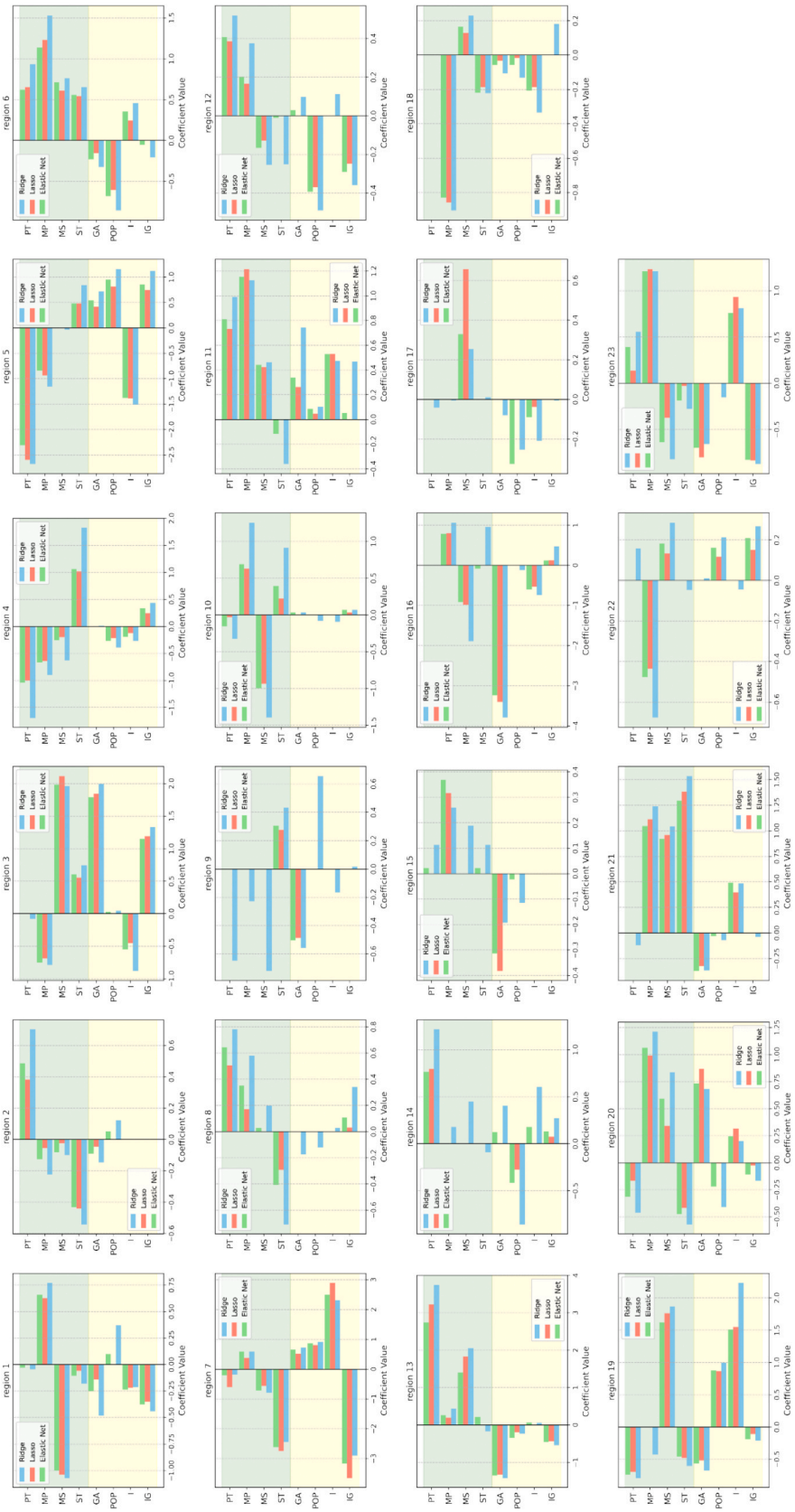

(caption on next page)

Fig. 13. The histogram illustrates the results of Ridge, Lasso, and Elastic Net regression analyses for groundwater storage (GWS) changes across 23 selected regions. In this chart, higher absolute values indicate a stronger influence of each factor on GWS. Green shading in the histogram represents the impact of climatic factors on GWS, while yellow shading denotes the influence of human factors. Mean Precipitation trend (mm/a): PT, Annual Mean Precipitation (mm/a): MP, SPEI trend: ST, mean SPEI: MS, Areas equipped for irrigation (%): I; Area equipped for irrigation with groundwater (%): IG, Population density (people/km^2): POP, Annual net abstraction from groundwater max value (mm/a): GA. (For interpretation of the references to colour in this figure legend, the reader is referred to the web version of this article.)

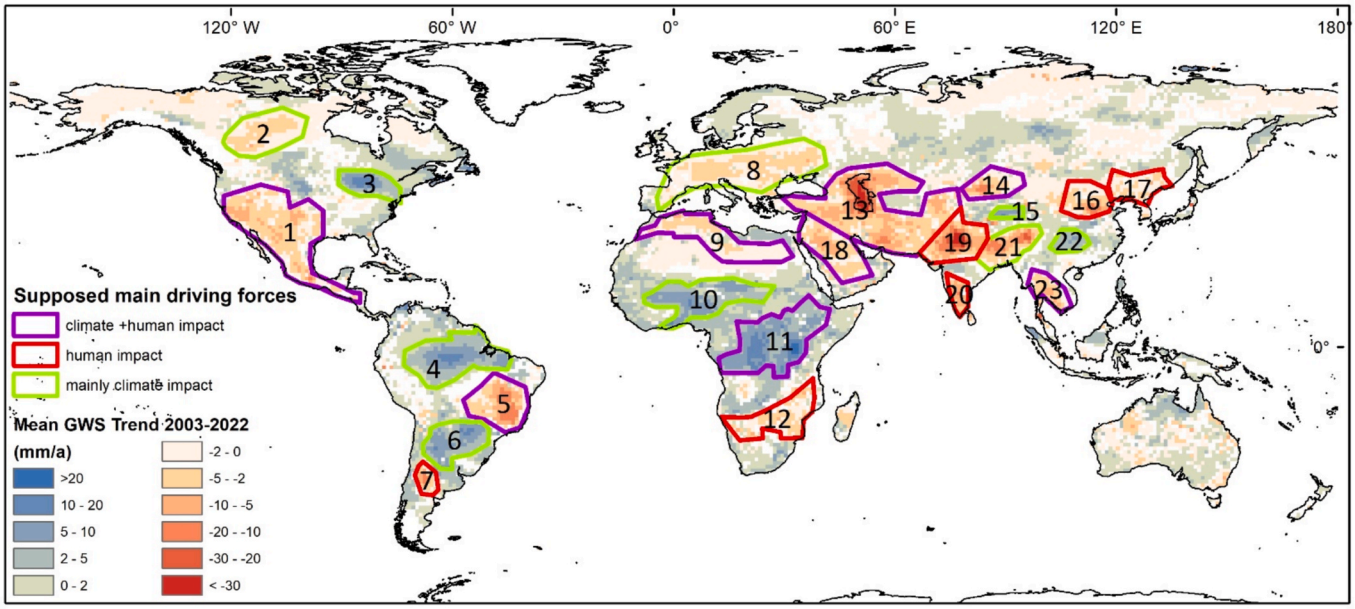

Fig. 14. The annotated map shows the 23 selected regions where significant changes in global groundwater storage occurred from 2003 to 2022, along with the supposed main driving forces behind these changes.

of arable land that primarily relies on rainfed agriculture. The annual average precipitation is low (195 mm/a), and the trend in precipitation is also declining, with a low leaf area index (LAI). Over the past 20 years, the SPEI Index has shown a drought trend towards.

The majority of lakes in the Tibetan Plateau (region 15) have increased in water level and extent during the 2000 s due to a combination of elevated precipitation rates and increased glacier-melt flows, which are difficult to disentangle (Zhang et al., 2013). Over the past 20 years, groundwater has been rising at a mean rate of 5.5 mm/a. There is no abstraction for agricultural irrigation in this region, thus the rise in GWS can be attributed to climate.

Numerous studies indicate a gradual GWS decline in the North China Plain (region 16) (e.g. Gong et al., 2018; Su et al., 2021). This region supports a large population of 209 million, with an average annual groundwater abstraction rate of 290 mm/a. The region surrounding Beijing heavily relies on extensive agriculture, which constitutes 44 % of the area. A significant portion of the water used for agriculture (30 %) comes from groundwater. The observed trend of groundwater depletion is primarily driven by excessive groundwater exploitation, a human-induced phenomenon likely to persist until groundwater scarcity or regulatory measures curtail consumption rates.

61 % of Northeast China (region 17) covered by agriculture, 36 % of irrigation comes from groundwater. The net abstraction from groundwater reaches a maximum of 69 mm/a, primarily supporting 137 million people and intense irrigation. During the GRACE period under consideration, the estimated mean rate of groundwater storage change was −1.7 mm/a, with a maximum of −5 mm/a. During this period, an increase in precipitation and a general wetting trend were observed. All available evidence suggests that the negative groundwater storage (GWS) trend is attributable to intensive agriculture and a high population density (Sun et al., 2022).

Decreasing water storage in the Arabian Peninsula (region 18) has been quantified using GRACE in previous studies (Joodaki et al., 2014; Voss et al., 2013). Over the past 20 years, most of the Arabian Peninsula has shown an increasing trend of aridity. The average groundwater storage (GWS) in this region is −2.9 mm/year, while precipitation, characteristic of a desert climate, averages 114 mm/year. Groundwater abstraction reaches a maximum of 169 mm/year, thus by far exceeding recharge rates and being not sustainable. This decline in groundwater storage is attributed to minimal rainfall and extensive groundwater extraction.

Over the past 20 years, Northern India (region 19) has experienced the most severe groundwater depletion globally (Asoka et al., 2017; Bhanja & Mukherjee, 2019). Despite an upward trend in precipitation and wetting trend in SPEI values, the substantial groundwater depletion trend persists. The average groundwater storage (GWS) in this region has decreased by −9.9 mm/a, with a maximum decline of −54.8 mm/a. The contribution of Himalayan glacier mass loss to this regional trend is minor (Tiwari et al., 2009; Rodell et al., 2018). Agriculture occupies 60 % of the area, with 37 % of irrigation relying on groundwater. Annual net abstraction from groundwater has reached 252 mm/a, exceeding the recharge rate, to support 566 million people and irrigation.

The groundwater storage in India exhibit distinct regional trends: a significant decline in the north, a rise in the central part, and a decreasing trend in Southern India (region 20). In the study by Asoka et al. (2017), southern India showed an increasing trend from 2002 to 2013. However, over the 20-year period from 2003 to 2022, groundwater storage (GWS) has exhibited a sharp decline, with an average decrease of −4.8 mm/a and a maximum decrease of −11.7 mm/a. In this region, groundwater abstraction reaches a maximum of 174 mm/a, with 58 % of the area relying on groundwater for irrigation, supporting 194 million population. The primary factors contributing to the groundwater decline include intensive agriculture (Salmon et al., 2015), significant groundwater extraction, and high population density, all of which result

in excessive groundwater withdrawal.

Approximately half of the South Asia (region 21) is devoted to irrigation. The region's highest net abstraction from groundwater is 238 mm/a, supporting irrigation agriculture and exceeding 478 million population and persistent groundwater withdrawal has led to a downward trend in groundwater levels. Despite the area's relatively abundant annual rainfall of approximately 1200 mm and its generally humid climate, the groundwater decline persists. The primary driver of this trend is the excessive water extraction driven by intensive agricultural activities and population density. The fact that extractions already exceed recharge during years of normal precipitation indicates a concerning outlook for groundwater availability during future drought (Aadhar & Mishra 2017).

Despite the dominance of rainfed agriculture (71 %) in Eastern Central China (region 22), groundwater storage has, on average, increased by 3.6 mm/a, with a maximum annual increase of 5.4 mm. This region also exhibits the largest positive trend in global precipitation, and the gradually increasing Standardized Precipitation Evapotranspiration Index (SPEI) may contribute to increased groundwater storage. Additionally, it is noteworthy that the construction and filling of the Three Gorges Dam (Yang & Lu 2014) have significantly contributed to the increase in groundwater storage (Chao et al., 2020; Yin et al., 2021).

In Mainland Southeast Asia (region 23), 50 % of the area is dedicated to agriculture, yet the water source for irrigation is rarely from groundwater. Overall, the region experiences abundant rainfall, averaging 1847 mm/a, with a rising precipitation trend at the rate of 2.12 mm/a over the past 20 years. Despite this, the mean groundwater storage (GWS) has the mean negative trend of −3.3 mm/a, with a maximum decline of −9.7 mm/a. This decline may be associated with climatic factors, such as the El Niño-Southern Oscillation (ENSO) (Sulaiman et al., 2023; Le et al., 2021) and intensity irrigation.

4. Conclusion

Groundwater is a critical component of land surface processes, playing a vital role in water and energy cycles. Moreover, it is an important source of drinking water supply and for agricultural irrigation. Thus, groundwater resources worldwide are impacted by climate change and human activities. This study utilized GRACE and ERA5-Land data to investigate groundwater storage variability from 2003 to 2022 at a 1° spatial resolution. GRACE data has revealed significant changes in global groundwater resources, allowing quantification at regional scales despite the limitations of sparse measurements and restrictive data-access policies.

Over the past two decades, groundwater storage has exhibited spatial heterogeneity, with most depletion occurring within the Earth's mid-latitudes. With a 95 % confidence level, approximately 81 % of global regions, excluding ice melt regions, have shown significant alterations in groundwater storage. Among these regions, 48 % have observed a decline in groundwater levels, while 52 % have recorded an increase. Approximately 3.4 billion people live in areas where groundwater has significantly declined over the past 20 years. Hotspots of groundwater storage (GWS) depletion, with significant declining trends (>20 mm/year), have been identified in northern India, eastern Brazil, and areas surrounding the Caspian Sea. These changes indicate a future where already limited groundwater resources will become increasingly valuable.

Spatial analysis revealed that the most significant groundwater declines occurred in arid and semi-arid regions, particularly where the aridity index (AI) ranges from 0.1 to 0.5, peaking at 0.1 to 0.2. These regions, characterized by sparse vegetation and fragile ecosystems, are experiencing declining groundwater storage. In contrast, groundwater storage is increasing in humid regions (AI $\geq$ 0.8). This disparity may lead to a more uneven distribution of groundwater.

Contrary to common belief, although there is a correlation between precipitation and groundwater storage (Thomas & Famiglietti 2019; Russo & Lall 2017), changes in precipitation do often not directly affect groundwater storage. Compared to precipitation, changes in the Standardized Precipitation-Evapotranspiration Index (SPEI) have a more significant spatial impact on groundwater storage, i.e. evapotranspiration and thus temperature play a vital role. While climate variability contributes to changes in water storage, human activities, particularly irrigation and excessive groundwater abstraction, are the major drivers of groundwater storage decline (Russo & Lall 2017). Among human activities, agricultural activities have a more significant impact on groundwater storage than population density. This may be due to the high demand for groundwater abstraction for agricultural irrigation, which is likely distributed in less populated areas (Chen et al., 2016). In contrast, groundwater use related to high population density, such as for drinking water, requires less groundwater. There are two main causes of groundwater rise: wetter climate conditions and dam construction. Reservoirs created by dam construction have led to significant groundwater rise in many regions, such as the Nile headwaters (Kebede et al., 2017), and Eastern Central China (Chao et al., 2020).

GRACE data transcends national borders and data confidentiality policies, enabling the study of terrestrial water storage (TWS) and groundwater storage (GWS) at global scale. Long-term monitoring with GRACE is essential for understanding large-scale groundwater storage trends. For instance, southern India showed an increasing trend in groundwater storage from 2002 to 2013 (Asoka et al., 2017), but it has since declined due to intensive agriculture and unreasonable abstraction from groundwater. Thus, continuous dynamic monitoring is crucial for developing effective groundwater management policies. Awareness of groundwater storage trends (Fig. 1) is the first step toward addressing the challenges through improved groundwater use efficiency and water management policies. Governments and planners in regions experiencing groundwater depletion can develop sustainable groundwater discharge and water conservation plans based on this information, promoting the sustainable use of freshwater resources.

CRediT authorship contribution statement

Jiawen Zhang: Writing – original draft, Validation, Software, Methodology, Formal analysis, Data curation, Conceptualization. **Tanja Liesch:** Writing – review & editing, Supervision, Software, Methodology, Conceptualization. **Nico Goldscheider:** Writing – review & editing, Supervision, Methodology, Conceptualization.

Funding

Jiawen Zhang is funded by the China Scholarship Council (202008220139).

Declaration of competing interest

The authors declare that they have no known competing financial interests or personal relationships that could have appeared to influence the work reported in this paper.

Data availability

No data was used for the research described in the article.

References

Aadhar, S., Mishra, V., 2017. High-resolution near real-time drought monitoring in South Asia. Sci. Data 4 (1), 1–14.

Ahmed, M., Sultan, M., Wahr, J., Yan, E., 2014. The use of GRACE data to monitor natural and anthropogenic induced variations in water availability across Africa. Earth Sci. Rev. 136, 289–300.

Alam, S., Gebremichael, M., Ban, Z., Scanlon, B.R., Senay, G., Lettenmaier, D.P., 2021. Post-drought groundwater storage recovery in California's Central Valley. Water Resour. Res. 57 (10), e2021WR030352.
Amanambu, A.C., Obarein, O.A., Mossa, J., Li, L., Ayeni, S.S., Balogun, O., Oyebamiji, A., Ochege, F.U., Ochege, F.U., 2020. Groundwater system and climate change: present status and future considerations. J. Hydrol. 589, 125163.
Anghileri, D., Botter, M., Castelletti, A., Weigt, H., Burlando, P., 2018. A comparative assessment of the impact of climate change and energy policies on Alpine hydropower. Water Resour. Res. 54 (11), 9144–9161.
Asoka, A., Gleeson, T., Wada, Y., Mishra, V., 2017. Relative contribution of monsoon precipitation and pumping to changes in groundwater storage in India. Nat. Geosci. 10 (2), 109–117.
Barichivich, J., Osborn, T., Harris, I., van der Schrier, G., Jones, P., 2019. Drought: monitoring global drought using the self-calibrating Palmer Drought Severity Index. Bull. Am. Meteorol. Soc. 100 (9), S39–S40.
Beguería, S., Vicente-Serrano, S.M., Reig, F., Latorre, B., 2014. Standardized precipitation evapotranspiration index (SPEI) revisited: parameter fitting, evapotranspiration models, tools, datasets and drought monitoring. Int. J. Climatol. 34 (10), 3001–3023.
Bhanja, S.N., Mukherjee, A., 2019. In situ and satellite-based estimates of usable groundwater storage across India: Implications for drinking water supply and food security. Adv. Water Resour. 126, 15–23.
Bhanja, S.N., Mukherjee, A., Rodell, M., 2020. Groundwater storage change detection from in situ and GRACE-based estimates in major river basins across India. Hydrol. Sci. J. 65 (4), 650–659.
Bhanja, S.N., Mukherjee, A., Saha, D., Velicogna, I., Famiglietti, J.S., 2016. Validation of GRACE based groundwater storage anomaly using in-situ groundwater level measurements in India. J. Hydrol. 543, 729–738.
Bouchard, F., Turner, K.W., MacDonald, L.A., Deakin, C., White, H., Farquharson, N., Medeiros, A.S., Wolfe, B.B., Hall, R.I., Pienitz, R., Edwards, T.W.D., 2013. Vulnerability of shallow subarctic lakes to evaporate and desiccate when snowmelt runoff is low. Geophys. Res. Lett. 40 (23), 6112–6117.
Brauman, K.A., Richter, B.D., Postel, S., Malsy, M., Flörke, M., 2016. Water depletion: an improved metric for incorporating seasonal and dry-year water scarcity into water risk assessments. Elementa 4, 000083.
Chao, N., Chen, G., Li, J., Xiang, L., Wang, Z., Tian, K., 2020. Groundwater storage change in the Jinsha River Basin from GRACE, hydrologic models, and in situ data. Groundwater 58 (5), 735–748.
Chen, J.L., Wilson, C.R., Tapley, B.D., 2010. The 2009 exceptional Amazon flood and interannual terrestrial water storage change observed by GRACE. Water Resour. Res. 46 (12).
Chen, J., Famigliett, J.S., Scanlon, B.R., Rodell, M., 2016. Groundwater storage changes: present status from GRACE observations. Remote Sens. Water Resour. 207–227.
Condon, L.E., Atchley, A.L., Maxwell, R.M., 2020. Evapotranspiration depletes groundwater under warming over the contiguous United States. Nat. Commun. 11 (1), 873.
Cuthbert, M.O., Taylor, R.G., Favreau, G., Todd, M.C., Shamsudduha, M., Villholth, K.G., Kukuric, N., 2019. Observed controls on resilience of groundwater to climate variability in sub-Saharan Africa. Nature 572 (7768), 230–234.
Dai, A., 2013. Increasing drought under global warming in observations and models. Nat. Clim. Chang. 3 (1), 52–58.
Döll, P., Müller Schmied, H., Schuh, C., Portmann, F.T., Eicker, A., 2014. Global-scale assessment of groundwater depletion and related groundwater abstractions: Combining hydrological modeling with information from well observations and GRACE satellites. Water Resour. Res. 50 (7), 5698–5720.
Dormann, C.F., Elith, J., Bacher, S., Buchmann, C., Carl, G., Carré, G., Lautenbach, S., 2013. Collinearity: a review of methods to deal with it and a simulation study evaluating their performance. Ecography 36 (1), 27–46.
Famiglietti, J.S., Lo, M., Ho, S.L., Bethune, J., Anderson, K.J., Syed, T.H., Rodell, M., 2011. Satellites measure recent rates of groundwater depletion in California's Central Valley. Geophys. Res. Lett. 38 (3).
Fan, X., Duan, Q., Shen, C., Wu, Y., Xing, C., 2020. Global surface air temperatures in CMIP6: Historical performance and future changes. Environ. Res. Lett. 15 (10), 104056.
Fan, Y., Li, H., Miguez-Macho, G., 2013. Global patterns of groundwater table depth. Science 339 (6122), 940–943.
Feng, W., Wang, C.Q., Mu, D.P., Zhong, M., Zhong, Y.L., Xu, H.Z., 2017. Groundwater storage variations in the North China Plain from GRACE with spatial constraints. Chin. J. Geophys. 60 (5), 1630–1642.
Gao, S., Hao, W., Fan, Y., Li, F., Wang, J., 2023. A multi-source GRACE fusion solution via uncertainty quantification of GRACE-derived terrestrial water storage (TWS) change. J. Geophys. Res.: Solid Earth 128 (11), e2023JB026908.
Gates, J.B., Scanlon, B.R., Mu, X., Zhang, L., 2011. Impacts of soil conservation on groundwater recharge in the semi-arid Loess Plateau, China. Hydrogeol. J. 4 (19), 865–875.
Gleeson, T., Wada, Y., Bierkens, M.F., Van Beek, L.P., 2012. Water balance of global aquifers revealed by groundwater footprint. Nature 488 (7410), 197–200.
Gong, H., Pan, Y., Zheng, L., Li, X., Zhu, L., Zhang, C., Zhou, C., 2018. Long-term groundwater storage changes and land subsidence development in the North China Plain (1971–2015). Hydrgeol. J. 26 (5), 1417–1427.
Green, T.R., Taniguchi, M., Kooi, H., Gurdak, J.J., Allen, D.M., Hiscock, K.M., Aureli, A., 2011. Beneath the surface of global change: Impacts of climate change on groundwater. J. Hydrol. 405 (3–4), 532–560.
Griffin, D., Anchukaitis, K.J., 2014. How unusual is the 2012–2014 California drought? Geophys. Res. Lett. 41 (24), 9017–9023.
Han, Z., Huang, S., Huang, Q., Leng, G., Wang, H., He, L., Li, P., 2019. Assessing GRACE-based terrestrial water storage anomalies dynamics at multi-timescales and their correlations with teleconnection factors in Yunnan Province, China. J. Hydrol. 574, 836–850.
Harris, I., Osborn, T.J., Jones, P., Lister, D., 2020. Version 4 of the CRU TS monthly high-resolution gridded multivariate climate dataset. Sci. Data 7 (1), 109.
Hassani, H. (2007). Singular spectrum analysis: methodology and comparison.
Heerspink, B.P., Kendall, A.D., Coe, M.T., Hyndman, D.W., 2020. Trends in streamflow, evapotranspiration, and groundwater storage across the Amazon Basin linked to changing precipitation and land cover. J. Hydrol.: Reg. Stud. 32, 100755.
Herbert, C., Döll, P., 2019. Global assessment of current and future groundwater stress with a focus on transboundary aquifers. Water Resour. Res. 55 (6), 4760–4784.
Herrera-Pantoja, M., Hiscock, K.M., 2008. The effects of climate change on potential groundwater recharge in Great Britain. Hydrol. Processes Int. J. 22 (1), 73–86.
Hirsch, R.M., Slack, J.R., Smith, R.A., 1982. Techniques of trend analysis for monthly water quality data. Water Resour. Res. 18 (1), 107–121.
Hoerl, A.E., Kennard, R.W., 1970. Ridge regression: Biased estimation for nonorthogonal problems. Technometrics 12 (1), 55–67.
Hu, Z., Chen, X., Zhou, Q., Yin, G., Liu, J., 2022. Dynamical variations of the terrestrial water cycle components and the influences of the climate factors over the Aral Sea Basin through multiple datasets. J. Hydrol. 604, 127270.
Ionita, M., Dima, M., Nagavciuc, V., Scholz, P., Lohmann, G., 2021. Past megadroughts in central Europe were longer, more severe and less warm than modern droughts. Commun. Earth Environ. 2 (1), 61.
Jacob, T., Wahr, J., Pfeffer, W.T., Swenson, S., 2012. Recent contributions of glaciers and ice caps to sea level rise. Nature 482 (7386), 514–518.
Jasechko, S., Perrone, D., 2021. Global groundwater wells at risk of running dry. Science 372 (6540), 418–421.
Jasechko, S., Seybold, H., Perrone, D., Fan, Y., Shamsudduha, M., Taylor, R.G., Kirchner, J.W., 2024. Rapid groundwater decline and some cases of recovery in aquifers globally. Nature 625 (7996), 715–721.
Joodaki, G., Wahr, J., Swenson, S., 2014. Estimating the human contribution to groundwater depletion in the Middle East, from GRACE data, land surface models, and well observations. Water Resour. Res. 50 (3), 2679–2692.
Jyolsna, P.J., Kambhammettu, B.V.N.P., Gorugantula, S., 2021. Application of random forest and multi-linear regression methods in downscaling GRACE derived groundwater storage changes. Hydrol. Sci. J. 66 (5), 874–887.
Kebede, S., Abdalla, O., Sefelnasr, A., Tindimugaya, C., Mustafa, O., 2017. Interaction of surface water and groundwater in the Nile River basin: isotopic and piezometric evidence. Hydrgeol. J. 25 (3), 707.
Keenan, T.F., Riley, W.J., 2018. Greening of the land surface in the world's cold regions consistent with recent warming. Nat. Clim. Chang. 8 (9), 825–828.
Kolusu, S.R., Shamsudduha, M., Todd, M.C., Taylor, R.G., Seddon, D., Kashaigili, J.J., MacLeod, D.A., 2019. The El Niño event of 2015–2016: climate anomalies and their impact on groundwater resources in East and Southern Africa. Hydrol. Earth Syst. Sci. 23 (3), 1751–1762.
Kutner, M. H. (2005). Applied linear statistical models.
Le, T., Ha, K.J., Bae, D.H., 2021. Projected response of global runoff to El Niño-Southern oscillation. Environ. Res. Lett. 16 (8), 084037.
Legg, S., 2021. IPCC, 2021: climate change 2021-the physical science basis. Interaction 49 (4), 44–45.
Li, B., Rodell, M., 2015. Evaluation of a model-based groundwater drought indicator in the conterminous US. J. Hydrol. 526, 78–88.
Li, W., Bao, L., Yao, G., Wang, F., Guo, Q., Zhu, J., Lu, S., 2024. The analysis on groundwater storage variations from GRACE/GRACE-FO in recent 20 years driven by influencing factors and prediction in Shandong Province, China. Scientific Reports 14 (1), 5819.
Li, W., Wang, W., Zhang, C., Wen, H., Zhong, Y., Zhu, Y., Li, Z., 2019. Bridging terrestrial water storage anomaly during GRACE/GRACE-FO gap using SSA method: a case study in China. Sensors 19 (19), 4144.
Lima, F.V., Gonçalves, R.M., Montecino, H.D., Carvalho, R.A., Mutti, P.R., 2022. Multi-sensor geodetic observations for drought characterization in the Northeast Atlantic Eastern Hydrographic Region, Brazil. Sci. Total Environ. 846, 157426.
Lin, Y.H., Lo, M.H., Chou, C., 2016. Potential negative effects of groundwater dynamics on dry season convection in the Amazon River basin. Clim. Dyn. 46, 1001–1013.
Marengo, J.A., Torres, R.R., Alves, L.M., 2017. Drought in Northeast Brazil—past, present, and future. Theor. Appl. Climatol. 129, 1189–1200.
Martens, B., Miralles, D.G., Lievens, H., van der Schalie, R., de Jeu, R.A.M., Fernández-Prieto, D., Beck, H.E., Dorigo, W.A., Verhoest, N.E.C., 2017. GLEAM v3: satellite-based land evaporation and root-zone soil moisture. Geosci. Model Dev. 10, 1903–1925. https://doi.org/10.5194/gmd-10-1903-2017.
Mekonnen, M.M., Hoekstra, A.Y., 2016. Four billion people facing severe water scarcity. Sci. Adv. 2 (2), e1500323.
Middleton, N. J., & Thomas, D. S. (Eds.). (1992). World atlas of desertification (pp. ix+-69).
Miralles, D.G., Holmes, T.R.H., de Jeu, R.A.M., Gash, J.H., Meesters, A.G.C.A., Dolman, A.J., 2011. Global land-surface evaporation estimated from satellite-based observations. Hydrol. Earth Syst. Sci. 15, 453–469. https://doi.org/10.5194/hess-15-453-2011.
Müller Schmied, H., Cáceres, D., Eisner, S., Flörke, M., Herbert, C., Niemann, C., Peiris, T. A., Popat, E., Portmann, F.T., Reinecke, R., Shadkam, S., Trautmann, T., Döll, P., 2021. The global water resources and use model WaterGAP v2. 2d: Model description and evaluation. Geosci. Model Dev. 14 (2), 1037–1079.
Müller, C., Elliott, J., Chryssanthacopoulos, J., Arneth, A., Balkovic, J., Ciais, P., Yang, H., 2017. Global gridded crop model evaluation: benchmarking, skills, deficiencies and implications. Geosci. Model Dev. 10 (4), 1403–1422.

Muñoz Sabater, J. (2019). ERA5-Land monthly averaged data from 1981 to present. Copernicus climate change service (C3S) climate data store (CDS), 10, 2025.
Muñoz-Sabater, J., Dutra, E., Agustí-Panareda, A., Albergel, C., Arduini, G., Balsamo, G., Thépaut, J.N., 2021. ERA5-Land: a state-of-the-art global reanalysis dataset for land applications. Earth Syst. Sci. Data 13 (9), 4349–4383.
Myneni, R., Knyazikhin, Y., & Park, T. (2021). MODIS/Terra Leaf Area Index/FPAR 8-Day L4 Global 500m SIN Grid V061. NASA EOSDIS Land Processes Distributed Active Archive Center (DAAC) data set, MOD15A2H-061.
Padrón, R.S., Gudmundsson, L., Decharme, B., Ducharne, A., Lawrence, D.M., Mao, J., Krinner, G., Kim, H., Seneviratne, S.I., 2020. Observed changes in dry-season water availability attributed to human-induced climate change. Nat. Geosci. 13 (7), 477–481.
Pointet, T., 2022. The United Nations world water development report 2022 on groundwater, a synthesis. Lhb 108 (1), 2090867.
Qadir, M., Noble, A. D., Qureshi, A. S., Gupta, R. K., Yuldashev, T., & Karimov, A. (2009). Salt-induced land and water degradation in the Aral Sea basin: A challenge to sustainable agriculture in Central Asia. In Natural Resources Forum (Vol. 33, No. 2, pp. 134-149). Oxford, UK: Blackwell Publishing Ltd.
Qi, W.Y., Chen, J., Li, L., Xu, C.Y., Li, J., Ang, Y., Zhang, S., 2022. Regionalization of catchment hydrological model parameters for global water resources simulations. Hydrol. Res. 53 (3), 441–466.
Rajaee, T., Ebrahimi, H., Nourani, V., 2019. A review of the artificial intelligence methods in groundwater level modeling. J. Hydrol. 572, 336–351.
Rateb, A., Scanlon, B.R., Pool, D.R., Sun, A., Zhang, Z., Chen, J., Zell, W., 2020. Comparison of groundwater storage changes from GRACE satellites with monitoring and modeling of major US aquifers. Water Resour. Res. 56 (12), e2020WR027556.
Rateb, A., Sun, A., Scanlon, B.R., Save, H., Hasan, E., 2022. Reconstruction of GRACE mass change time series using a Bayesian framework. Earth Space Sci. 9 (7), e2021EA002162.
Richey, A.S., Thomas, B.F., Lo, M.H., Reager, J.T., Famiglietti, J.S., Voss, K., Rodell, M., 2015. Quantifying renewable groundwater stress with GRACE. Water Resour. Res. 51 (7), 5217–5238.
Rodell, M., Famiglietti, J.S., Wiese, D.N., Reager, J.T., Beaudoing, H.K., Landerer, F.W., Lo, M.H., 2018. Emerging trends in global freshwater availability. Nature 557 (7707), 651–659.
Rodell, M., Velicogna, I., Famiglietti, J.S., 2009. Satellite-based estimates of groundwater depletion in India. Nature 460 (7258), 999–1002.
Rohde, M.M., Albano, C.M., Huggins, X., Klausmeyer, K.R., Morton, C., Sharman, A., Stella, J.C., 2024. Groundwater-dependent ecosystem map exposes global dryland protection needs. Nature 632 (8023), 101–107.
Russo, T.A., Lall, U., 2017. Depletion and response of deep groundwater to climate-induced pumping variability. Nat. Geosci. 10 (2), 105–108.
Salmon, J.M., Friedl, M.A., Frolking, S., Wisser, D., Douglas, E.M., 2015. Global rain-fed, irrigated, and paddy croplands: a new high resolution map derived from remote sensing, crop inventories and climate data. Int. J. Appl. Earth Obs. Geoinf. 38, 321–334.
Santos, E.B., de Freitas, E.D., Rafee, S.A.A., Fujita, T., Rudke, A.P., Martins, L.D., Martins, J.A., 2021. Spatio-temporal variability of wet and drought events in the Paraná River basin—Brazil and its association with the El Niño—Southern oscillation phenomenon. Int. J. Climatol. 41, 4879–4897.
Satizábal-Alarcón, D.A., Suhogusoff, A., Ferrari, L.C., 2024. Characterization of groundwater storage changes in the Amazon River Basin based on downscaling of GRACE/GRACE-FO data with machine learning models. Sci. Total Environ. 912, 168958.
Save, H. (2020). Csr grace and grace-fo rl06 mascon solutions v02. University of Texas at Austin, 1.
Save, H., Bettadpur, S., Tapley, B.D., 2016. High-resolution CSR GRACE RL05 mascons. J. Geophys. Res. Solid Earth 121 (10), 7547–7569.
Scanlon, B.R., Fakhreddine, S., Rateb, A., de Graaf, I., Famiglietti, J., Gleeson, T., Zheng, C., 2023. Global water resources and the role of groundwater in a resilient water future. Nat. Rev. Earth Environ. 4 (2), 87–101.
Scanlon, B.R., Rateb, A., Anyamba, A., Kebede, S., MacDonald, A.M., Shamsudduha, M., Small, J., Sun, A., Taylor, R.G., Xie, H., 2022. Linkages between GRACE water storage, hydrologic extremes, and climate teleconnections in major African aquifers. Environ. Res. Lett. 17 (1), 014046.
Scanlon, B.R., Zhang, Z., Save, H., Sun, A.Y., Müller Schmied, H., Van Beek, L.P., Bierkens, M.F., 2018. Global models underestimate large decadal declining and rising water storage trends relative to GRACE satellite data. Proc. Natl. Acad. Sci. 115 (6), E1080–E1089.
Seidou, O., Asselin, J.J., Ouarda, T.B., 2007. Bayesian multivariate linear regression with application to change point models in hydrometeorological variables. Water Resour. Res. 43 (8).
Sen, P.K., 1968. Estimates of the regression coefficient based on Kendall's tau. J. Am. Stat. Assoc. 63 (324), 1379–1389.
Setegn, S.G., Rayner, D., Melesse, A.M., Dargahi, B., Srinivasan, R., 2011. Impact of climate change on the hydroclimatology of Lake Tana Basin, Ethiopia. Water Resour. Res. 47 (4).
Shamsudduha, M., Taylor, R.G., 2020. Groundwater storage dynamics in the world's large aquifer systems from GRACE: uncertainty and role of extreme precipitation. Earth Syst. Dyn. 11 (3), 755–774.
Siebert, S., Burke, J., Faures, J.M., Frenken, K., Hoogeveen, J., Döll, P., Portmann, F.T., 2010. Groundwater use for irrigation–a global inventory. Hydrol. Earth Syst. Sci. 14 (10), 1863–1880.
Siebert, S., Henrich, V., Frenken, K., & Burke, J. (2013). Update of the digital global map of irrigation areas to version 5. Rheinische Friedrich-Wilhelms-Universität, Bonn, Germany and Food and Agriculture Organization of the United Nations, Rome, Italy, 10(2.1), 2660-6728.
Song, X.P., Hansen, M.C., Stehman, S.V., Potapov, P.V., Tyukavina, A., Vermote, E.F., Townshend, J.R., 2018. Global land change from 1982 to 2016. Nature 560 (7720), 639–643.
Spinoni, J., Barbosa, P., De Jager, A., McCormick, N., Naumann, G., Vogt, J.V., Mazzeschi, M., 2019a. A new global database of meteorological drought events from 1951 to 2016. J. Hydrol.: Reg. Stud. 22, 100593.
Spinoni, J., Barbosa, P., De Jager, A., McCormick, N., Naumann, G., Vogt, J.V., Magni, D., Masante, D., Mazzeschi, M., 2019b. A new global database of meteorological drought events from 1951 to 2016. J. Hydrol.: Reg. Stud. 22, 100593.
Su, G., Wu, Y., Zhan, W., Zheng, Z., Chang, L., Wang, J., 2021. Spatiotemporal evolution characteristics of land subsidence caused by groundwater depletion in the North China plain during the past six decades. J. Hydrol. 600, 126678.
Sulaiman, A., Osaki, M., Takahashi, H., Yamanaka, M.D., Susanto, R.D., Shimada, S., Tsuji, N., 2023. Peatland groundwater level in the Indonesian maritime continent as an alert for El Niño and moderate positive Indian Ocean dipole events. Sci. Rep. 13 (1), 939.
Sun, Q., Xu, C., Gao, X., Lu, C., Cao, B., Guo, H., He, X., 2022. Response of groundwater to different water resource allocation patterns in the Sanjiang Plain, Northeast China. J. Hydrol.: Reg. Stud. 42, 101156.
Sun, Z., Long, D., Yang, W., Li, X., Pan, Y., 2020. Reconstruction of GRACE data on changes in total water storage over the global land surface and 60 basins. Water Resour. Res. 56 (4), e2019WR026250.
Sutanudjaja, E.H., Van Beek, R., Wanders, N., Wada, Y., Bosmans, J.H., Drost, N., Bierkens, M.F., 2018. PCR-GLOBWB 2: a 5 arcmin global hydrological and water resources model. Geosci. Model Dev. 11 (6), 2429–2453.
Tabari, H., 2020. Climate change impact on flood and extreme precipitation increases with water availability. Sci. Rep. 10 (1), 13768.
Tao, F., Chen, Y., Fu, B., 2020. Impacts of climate and vegetation leaf area index changes on global terrestrial water storage from 2002 to 2016. Sci. Total Environ. 724, 138298.
Taylor, R.G., Scanlon, B., Döll, P., Rodell, M., Van Beek, R., Wada, Y., Treidel, H., 2013. Ground water and climate change. Nat. Clim. Chang. 3 (4), 322–329.
Thomas, B.F., Famiglietti, J.S., 2019. Identifying climate-induced groundwater depletion in GRACE observations. Sci. Rep. 9 (1), 4124.
Thomas, B.F., Caineta, J., Nanteza, J., 2017. Global assessment of groundwater sustainability based on storage anomalies. Geophys. Res. Lett. 44 (22), 11–445.
Tibshirani, R., 1996. Regression shrinkage and selection via the lasso. J. R. Stat. Soc. Ser. B Stat Methodol. 58 (1), 267–288.
Tiwari, V.M., Wahr, J., Swenson, S., 2009. Dwindling groundwater resources in northern India, from satellite gravity observations. Geophys. Res. Lett. 36 (18).
Van Lanen, H.A., Laaha, G., Kingston, D.G., Gauster, T., Ionita, M., Vidal, J.P., Van Loon, A.F., 2016. Hydrology needed to manage droughts: the 2015 European case. Hydrol. Process. 30 (17), 3097–3104.
Van Loon, A.F., 2015. Hydrological drought explained. Wiley Interdiscip. Rev. Water 2 (4), 359–392.
Vautard, R., Yiou, P., Ghil, M., 1992. Singular-spectrum analysis: a toolkit for short, noisy chaotic signals. Physica D 58 (1–4), 95–126.
Veldkamp, T.I.E., Zhao, F., Ward, P.J., De Moel, H., Aerts, J.C., Schmied, H.M., Wada, Y., 2018. Human impact parameterizations in global hydrological models improve estimates of monthly discharges and hydrological extremes: a multi-model validation study. Environ. Res. Lett. 13 (5), 055008.
Velicogna, I., Sutterley, T.C., Van Den Broeke, M.R., 2014. Regional acceleration in ice mass loss from Greenland and Antarctica using GRACE time-variable gravity data. Geophys. Res. Lett. 41 (22), 8130–8137.
Vicente-Serrano, S.M., Beguería, S., López-Moreno, J.I., 2010. A multiscalar drought index sensitive to global warming: the standardized precipitation evapotranspiration index. J. Clim. 23 (7), 1696–1718.
Voss, K.A., Famiglietti, J.S., Lo, M., De Linage, C., Rodell, M., Swenson, S.C., 2013. Groundwater depletion in the Middle East from GRACE with implications for transboundary water management in the Tigris-Euphrates-Western Iran region. Water Resour. Res. 49 (2), 904–914.
Wada, Y., Wisser, D., Bierkens, M.F., 2014. Global modeling of withdrawal, allocation and consumptive use of surface water and groundwater resources. Earth Syst. Dyn. 5 (1), 15–40.
Wang, L., Zhang, Y., 2024. Filling GRACE data gap using an innovative transformer-based deep learning approach. Remote Sens. Environ. 315, 114465.
Wang, W., Zhu, Y., Xu, R., Liu, J., 2015. Drought severity change in China during 1961–2012 indicated by SPI and SPEI. Nat. Hazards 75, 2437–2451.
Wiese, D.N., Landerer, F.W., Watkins, M.M., 2016. Quantifying and reducing leakage errors in the JPL RL05M GRACE mascon solution. Water Resour. Res. 52 (9), 7490–7502.
Williams, A.P., Cook, E.R., Smerdon, J.E., Cook, B.I., Abatzoglou, J.T., Bolles, K., Livneh, B., 2020. Large contribution from anthropogenic warming to an emerging north American megadrought. Science 368 (6488), 314–318.
WorldPop. (2018). Global high resolution population denominators Project - funded by the bill and melinda gates foundation (OPP1134076). Columbia University. https://doi.org/10.5258/SOTON/WP00670. School of Geography and Environmental Science, University of Southampton; Department of Geography and Geosciences, University of Louisville; Departement de Geographie, Universite de Namur and Center for International Earth Science Information Network (CIESIN) www.worldpop.org.
Xanke, J., Liesch, T., 2022. Quantification and possible causes of declining groundwater resources in the Euro-Mediterranean region from 2003 to 2020. Hydrgeol. J. 30 (2), 379–400.

Yang, X., Lu, X., 2014. Drastic change in China's lakes and reservoirs over the past decades. Sci. Rep. 4 (1), 6041.
Yi, S., Sneeuw, N., 2021. Filling the data gaps within GRACE missions using singular spectrum analysis. J. Geophys. Res. Solid Earth 126 (5), e2020JB021227.
Yilmaz, I., Yuksek, A.G., 2008. An example of artificial neural network (ANN) application for indirect estimation of rock parameters. Rock Mech. Rock Eng. 41 (5), 781.
Yin, W., Zhang, G., Han, S.C., Yeo, I.Y., Zhang, M., 2022. Improving the resolution of GRACE-based water storage estimates based on machine learning downscaling schemes. J. Hydrol. 613, 128447.
Yin, Z., Xu, Y., Zhu, X., Zhao, J., Yang, Y., Li, J., 2021. Variations of groundwater storage in different basins of China over recent decades. J. Hydrol. 598, 126282.
Yira, Y., Diekkrüger, B., Steup, G., Bossa, A.Y., 2016. Modeling land use change impacts on water resources in a tropical West African catchment (Dano, Burkina Faso). J. Hydrol. 537, 187–199.
Zarfl, C., Lumsdon, A.E., Berlekamp, J., Tydecks, L., Tockner, K., 2015. A global boom in hydropower dam construction. Aquat. Sci. 77, 161–170.
Zhang, G., Xu, T., Yin, W., Bateni, S.M., Jun, C., Kim, D., Liu, S., Xu, Z., Ming, W., Wang, J., 2024. A machine learning downscaling framework based on a physically constrained sliding window technique for improving resolution of global water storage anomaly. Remote Sens. Environ. 313, 114359.
Zhang, T.Y., Jin, S.G., 2013. Estimate of glacial isostatic adjustment uplift rate in the Tibetan Plateau from GRACE and GIA models. J. Geodyn. 72, 59–66.
Zhang, X., Li, J., Dong, Q., Wang, Z., Zhang, H., Liu, X., 2022. Bridging the gap between GRACE and GRACE-FO using a hydrological model. Sci. Total Environ. 822, 153659.
Zou, H., Hastie, T., 2005. Regularization and variable selection via the elastic net. J. R. Stat. Soc. Ser. B Stat Methodol. 67 (2), 301–320.